Pergamon

Geochimica et Cosmochimica Acta, Vol. 66, No. 20, pp. 3615–3633, 2002

0016-7037/02 $22.00 + .00

PII S0016-7037(02)00942-0

A spectrophotometric study of aqueous copper(I)–chloride complexes in LiCl solutions between 100 °C and 250 °C

WEIHUA LIU,[1,*] JOËL BRUGGER,[1,†] D. C. MCPHAIL[1,#] and LEONE SPICCIA[2]

[1]School of Geosciences, P. O. Box 28E, Monash University, Victoria 3800, Australia
[2]School of Chemistry, P. O. Box 23, Monash University, Victoria 3800, Australia

(*Received August* 10, 2001; *accepted in revised form May* 1, 2002)

Abstract—Copper transport and deposition in highly saline hydrothermal fluids are controlled by the stability of copper(I) complexes with ligands such as chloride and hydrosulphide. However, our understanding of the behavior of copper(I)–chloride complexes at elevated temperatures and in highly saline brines is limited by the conditions of existing experimental studies where the maximum chloride concentration is 2 m. This paper presents the results of a study of copper(I)–chloride complexes at much higher chloride concentrations, 1.5 m to 9.1 m, using a UV spectrophotometric method. The UV spectra of copper(I)-bearing LiCl solutions were measured at temperatures between 100 °C and 250 °C at vapor-saturated pressures and quantitative interpretation of the spectra shows that $CuCl_2^-$, $CuCl_3^{2-}$, and $CuCl_4^{3-}$ were present in the experimental solutions. The fitted logarithms of formation constants (log *K*) for $CuCl_2^-$ are in good agreement with the previous results of solubility experiments reported by Xiao et al. (1998) and Liu et al. (2001). The log *K* values for $CuCl_3^{2-}$ also agree with those of Liu et al. (2001) and theoretical estimates of Sverjensky et al. (1997). This study presents the first experimentally determined formation constants for $CuCl_4^{3-}$, at temperatures greater than 25 °C, and indicates that this complex predominates at chloride concentrations greater than 5 m. Based on the new log *K* values generated from this study, the calculated chalcopyrite solubility in NaCl solutions indicates that in addition to cooling, fluid mixing (dilution of saline fluids) may be an important factor controlling the deposition of copper minerals from hydrothermal solutions.

1. INTRODUCTION

Hydrothermal copper deposits contain most of the world's copper reserves, and form under a wide variety of geological, chemical, and physical conditions. Copper is transported in hydrothermal fluids mainly in reduced form [copper(I)] and its transport in mineralizing fluids has been mainly attributed to copper(I)–chloride (e.g., Liu et al., 2001) and copper(I)–bisulfide complexes (e.g., Mountain and Seward, 1999). Despite the likely importance of copper(I)–chloride complexes in ore-forming hydrothermal fluids, geothermal systems and some industrial processes, the thermodynamic properties of these aqueous complexes at elevated temperature and high chloride concentrations are still poorly known, thereby limiting our understanding of copper transport and deposition in hydrothermal environments.

Many experimental studies have been conducted at room temperature to investigate copper(I)–chloride complexes in aqueous solutions. The dominant copper(I)–chloride complexes and their formation constants have been derived from solubility, potentiometric, and spectrophotometric measurements (e.g., Glasner and Avinur, 1961; Sukhova et al., 1968; Ahrland and Rawsthorne, 1970; Hikita et al., 1973; Sugasaka and Fujii, 1976; Davis et al., 1978; Fritz, 1980; Sharma and Millero, 1990; Ciavatta and Iuliano, 1998).

There have been fewer studies of copper(I)–chloride complexes at high temperatures, where only mineral solubility methods have been used (Crerar and Barnes, 1976; Hemley et al., 1992; Var'yash, 1992; Seyfried and Ding, 1993, 1995; Xiao et al., 1998; Liu et al., 2001). The conclusions differ in terms of the nature of the predominant complexes and the value of their formation constants. A limitation of existing high-temperature solubility studies is that the chloride concentration has usually been less than 1 m (i.e., 5.5 wt. % NaCl), which is not high enough to identify copper(I)–chloride complexes likely to be present in the high salinity ore-forming hydrothermal fluids associated with the most common types of copper deposits (Fig. 1). For example, high-temperature (>450 °C) porphyry deposits contain up to 55 wt. % NaCl equivalent (e.g., Roedder, 1984; Hezarkhani and Williams-Jones, 1998; Ulrich et al., 1999), and low temperature (<200 °C) sediment-hosted deposits contain up to 20 wt. % NaCl equivalent (Haynes, 1986; Ran et al., 1995). Recently, Liu et al. (2001) reported the results of a cuprite solubility study of copper(I)–chloride complexes in 0.001–2 m NaCl solutions at temperatures between 50 °C and 250 °C. The formation constants for $CuCl_{(aq)}$ and $CuCl_2^-$ derived from that study are in agreement with those of Xiao et al. (1998); however, deriving reliable formation constants for $CuCl_3^{2-}$ is more problematic. Although Xiao et al. (1998) presented formation constants for $CuCl_3^{2-}$, Liu et al. (2001) could not obtain reliable formation constants for $CuCl_3^{2-}$ at temperatures greater than 50 °C, a complex that is likely to become important at chloride concentrations greater than 2 m. The high solubility of cuprite prevented Liu et al. (2001) from extending their investigation to higher chloride concentrations because the buffer capacity of the acetic acid–sodium acetate *p*H buffer used in their experiments was exceeded. Another problem associated with high solubilities is the likely occur-

* *Present address:* CSIRO Exploration and Mining, P. O. Box 136, North Ryde, NSW 1670, Australia. (weihua.liu@csiro.au).
† *Present address:* South Australian Museum and University of Adelaide, North Terrace, SA 5000, Australia.
# *Present address:* Department of Geology, Australian National University, ACT 0200, Australia.

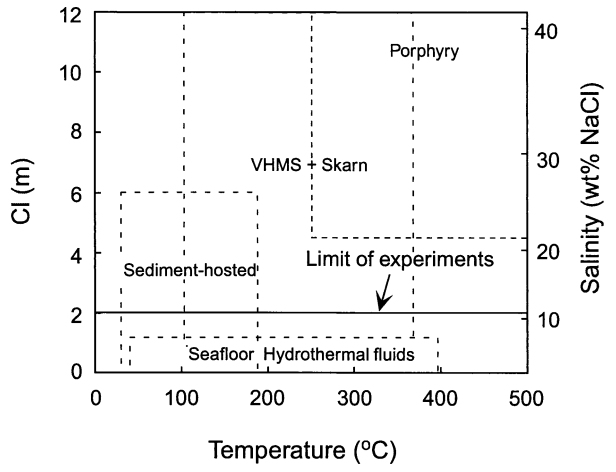

Fig. 1. Approximate salinity vs. temperature ranges for various copper ore-forming environments. The ranges are estimated from fluid inclusion data of Roedder (1984), Haynes (1986), Ran et al. (1995), Hezarkhani and Williams-Jones (1998), and Ulrich et al. (1999). The estimates for seafloor hydrothermal systems are based on Hannington et al. (1995) and Von Damm (1995). The solid line shows the upper limit of chloride concentration used in copper(I)-bearing experiments.

rence of polynuclear Cu(I) complexes, which are difficult to detect in solubility experiments, and which make data interpretation more difficult. Thus, the existence and properties of $CuCl_3^{2-}$ and other possible copper(I)–chloride complexes in brines with higher chloride concentrations at elevated temperatures still need to be investigated.

The solubility method used in the above studies is a good technique to investigate heterogeneous systems (mineral + brine), useful if not necessary in deriving reliable thermodynamic properties for solubility reactions, but its use is often limited by high solubilities of minerals at high temperature and salinity. The ultraviolet–visible spectrophotometric technique complements the solubility method for investigation of aqueous metal chloride complexes at elevated temperatures and has several advantages: (i) it provides for a direct *in situ* measurement of the electronic spectra of metal complexes at elevated temperatures; (ii) it provides information about the structure of aqueous complexes; and more importantly (iii) chloride concentrations are not limited by high mineral solubility. This means we can investigate metal chloride complexes at much higher salinity than can be used in direct solubility experiments and furthermore the results provide an independent check on the results of solubility studies.

The aims of this study are to identify the copper(I)–chloride complexes present in aqueous solutions containing chloride concentrations higher than can be used in solubility experiments at elevated temperatures, measure the thermodynamic properties of those complexes, and show the effects on copper mineral solubilities over wide ranges in temperature and chloride concentration. We present the results of a ultraviolet spectrophotometric study of copper(I)–chloride complexes in aqueous LiCl solutions (1.5–9.1 m) at temperatures between 100 °C and 250 °C. LiCl was chosen because of its high solubility at room temperature and mean stoichiometric activity coefficient data are available for LiCl solutions up to 250 °C (Holmes and Mesmer, 1983). The combination of new and existing thermodynamic properties enables us to quantify copper transport in hydrothermal brines and waters for the wide ranges of salinity and temperature conditions found in geological environments.

Table 1. Total chloride and copper concentrations of sample solutions used in the measurement of UV spectra.

	Copper concentration (ppm)	
$[Cl]_{total\ (m)}$	100–200 °C	250 °C
1.456	21.97	21.97
1.916	21.83	21.83
2.372	21.05	21.05
2.900	18.95	18.95
2.960	17.16	17.16
3.299	25.13	
3.709	17.31	17.31
3.830		20.44
3.986	17.59	
4.774	18.07	18.07
5.867	17.16	17.16
6.815	13.62	13.62
7.860	12.47	12.47
9.102	11.43	11.43

2. EXPERIMENTAL METHODS

2.1. Solution Preparation

The total chloride and copper concentrations in solutions used to measure UV spectra are listed in Table 1. Since copper(I) is readily oxidized to copper(II) in the presence of oxygen, solutions were prepared in a glove box under a nitrogen atmosphere. All solutions were prepared by weight using reagent-grade chemicals and freshly boiled, doubly deionized water. Copper(I)–chloride salt ($CuCl_{(s)}$) was prepared according to the procedure of Keller and Wycoff (1946). Copper(I)–chloride stock solutions were prepared by dissolving appropriate quantities of $CuCl_{(s)}$ in 2 m LiCl solutions to yield copper concentrations of 250–300 ppm. In the presence of 2 m LiCl, copper(I) solutions were found to be stable (i.e., no oxidation) for up to one month in a glove box filled with nitrogen gas. In contrast, copper(I) solutions prepared in 1 m LiCl were stable for approximately one week before a blue color, indicative of the presence of Cu(II), became apparent. A small quantity of weighed stock solution (approximately 1–3 g) was added into each weighed sample solution (40–60 g) with LiCl concentrations between 1.5 m and 9.1 m to give copper concentrations of 11–25 ppm (Table 1). Solutions were acidified with hydrochloric acid to prevent hydrolyzed complexes, resulting in measured *p*H values between 3.20 and 3.98. Copper concentrations of stock and sample solutions were checked using a neocuproine spectrophotometric method (Gahler, 1954). The amount of copper(II) presented in the solutions was negligible ($<<$1%) based on the lack of absorption characteristics of copper(II) complexes at characteristic UV–vis wavelengths known from previous studies (e.g., Davis et al., 1978; Brugger et al., 2001).

2.2. High-Temperature UV Spectra Measurements

A high-temperature titanium (Commercially pure Grade VII) optical cell fitted with UV transparent sapphire windows was used to measure UV–vis absorption at all temperatures. The cell is a cylinder with 95 mm outer diameter and 90 mm height, and the optical path length through the sample is 50 mm. The volume of the sample chamber is approximately 27 cm^3. Each solution (approximately 16 cm^3) was loaded into the cell with a Teflon syringe in a glove box under a nitrogen atmosphere. In the cell, the solution was only in contact with titanium and sapphire windows. The cell was enclosed in a circular heating jacket and then mounted in the sample compartment of a Varian Cary 5G spectrophotometer. The temperature was controlled with a type *K* thermocouple inserted in a thermocouple well drilled into

the top of the cell and an automated temperature controller. The bottom of that thermocouple well is about 60 mm from the top of the cell, and about 17.5 mm from the solution. A second thermocouple was located in a well on the opposite side of the cell, at a similar distance from the solution, but the bottom of this well is only 23 mm from the top of the cell. The two thermocouples therefore bracket the sample compartment of the cell. The temperature difference between the thermocouples was within 1 °C, and any temperature gradients in the cell were ignored.

For each solution, spectra of a copper-free blank solution containing the same concentration of LiCl and HCl were measured before the measurement of the copper-bearing sample solution. These baseline spectra were subtracted from the spectra of the sample solutions in order to correct the spectra for detector responses, and for absorption by the windows and the LiCl solutions. All spectra were measured with 1 nm increments between 200 nm and 400 nm and collected at temperatures of 25 °C, 50 °C, 100 °C, 150 °C, 200 °C, and 250 °C during heating. Usually the absorption stabilized within a few minutes after the temperature had stabilized, although measurements were usually taken 20 minutes later. The data collected at 25 °C and 50 °C were not used for interpretation because the absorption of the most sample solutions at these two temperatures exceeded the machine limit (~4 absorbance units) and were thus unreliable. The absorption spectra measured at the higher temperatures (100–250 °C) were typically in the range of 1–3 absorbance units. Within this range the analytical uncertainties of the spectrophotometer is about 0.005 absorbance unit, i.e., 0.5% for an absorbance of 1.

Spectra were also measured during cooling for many sample solutions in order to check for possible leaks, oxidation of copper(I) and precipitation during the experiment. The differences between the spectra collected at the same temperature during heating and cooling cycles were within 0.02 and 0.05 absorbance units at 150 °C and 100 °C, respectively. This indicates no significant loss of copper(I) in the solutions after cooling from 250 °C.

3. RESULTS AND QUALITATIVE ANALYSIS

Figure 2a shows typical UV spectra of lithium chloride solutions containing no cuprous chloride. These spectra show that the absorption observed at some wavelengths (i.e., 200 nm) at 25 °C undergoes substantial redshift with increasing temperature. This absorption is attributed to a charge-transfer-to-solvent (CCTS) transition as discussed by Seward (1984) and Bebie et al. (1998). The net result of this effect is a reduction in the range of wavelength for which useful information about copper(I)–chloride complexes can be gained, especially with increasing temperature.

Prior to interpretation of the spectra, data for solutions containing copper(I) chloride have to be converted to a molarity scale, on which the Beer–Lambert law is based. The molar to molal transfer factor for LiCl solution is expressed by (e.g., Heinrich and Seward, 1990)

$$f_s = \frac{1000 + W_{\mathrm{LiCl}} m_{\mathrm{LiCl}}}{1000 \rho_{\mathrm{LiCl}(m_{\mathrm{LiCl}}, T)}}, \qquad (1)$$

where W_{LiCl} is the molecular mass of LiCl, m_{LiCl} is the total molality of LiCl in the solution, and $\rho_{\mathrm{LiCl}(m_{\mathrm{LiCl}}, T)}$ refers to the density (g/cm^3) of LiCl solutions at temperature T. The densities of LiCl–H_2O mixtures measured by Majer et al. (1989) at temperatures of 50–277 °C and LiCl concentrations of 0.05–3 m were interpolated to temperatures used in this study and then extrapolated to 9 m LiCl by polynomial regression, as in Heinrich and Seward (1990). The resulting equations for $\rho_{\mathrm{LiCl}(m_{\mathrm{LiCl}}, T)}$, used in Eqn. 1, are shown in Table 2. The influence of uncertainties of density on the molar absorbance is insignificant because the correction of Eqn. 1 is small, as suggested by Heinrich and Seward (1990).

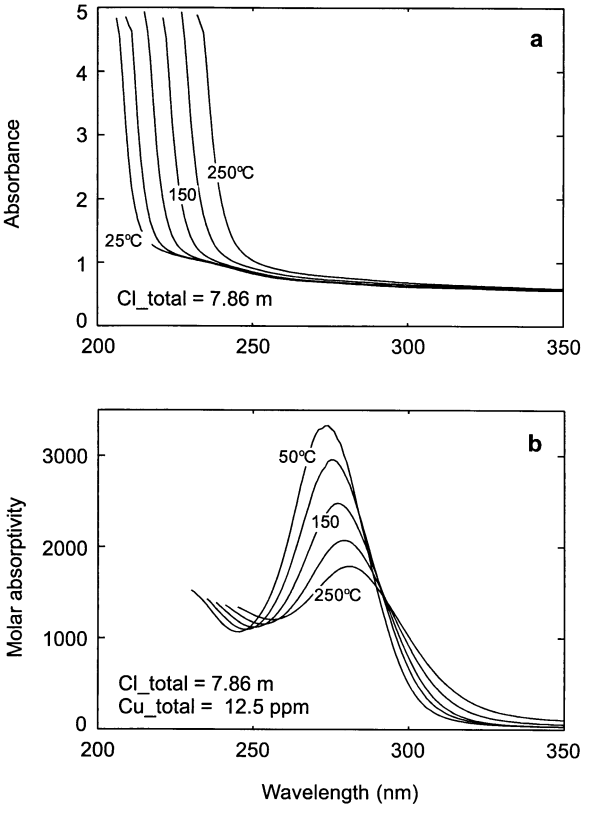

Fig. 2. UV spectra for LiCl and CuCl + LiCl solutions: (a) absorbance of 7.86 m LiCl with no copper solution at 25 °C, 50 °C, 100 °C, 150 °C, 200 °C, and 250 °C—path length = 50 mm; (b) apparent molar absorptivity spectra of a 12.5 ppm Cu + 7.86 m LiCl solution at temperatures between 50 °C and 250 °C (50 °C increments).

The temperature dependence of the apparent molar absorptivity spectra [obtained by applying the Beer–Lambert law and using the total copper concentration (M) and a path length of 5 cm] for a typical sample solution is shown in Figure 2b. The spectra for other sample solutions with different chloride concentrations show the same temperature dependence. First, there is a single absorption peak in the 260–280 nm range and a shoulder at wavelengths lower than 250 nm. The absorption maximum at 50 °C is at 274 nm, in good agreement with previous room temperature studies (Sugasaka and Fujii, 1976; Davis et al., 1978; Sharma and Millero, 1990). With increasing temperature, the position of the absorption maximum shifts towards lower energy (276 nm at 150 °C and 279 nm at 250

Table 2. Equations for density (ρ) obtained by polynomial regression of the density data reported by Majer et al. (1989) for LiCl solution (m refers to total molality of LiCl).

T (°C)	ρ (g/cm^3)
50	$0.9886 + 0.024\,16m - 0.000\,868m^2$
100	$0.9563 + 0.026\,25m - 0.000\,986m^2$
150	$0.9171 + 0.029\,97m - 0.001\,268m^2$
200	$0.8635 + 0.035\,57m - 0.001\,761m^2$
250	$0.7965 + 0.045\,10m - 0.002\,810m^2$

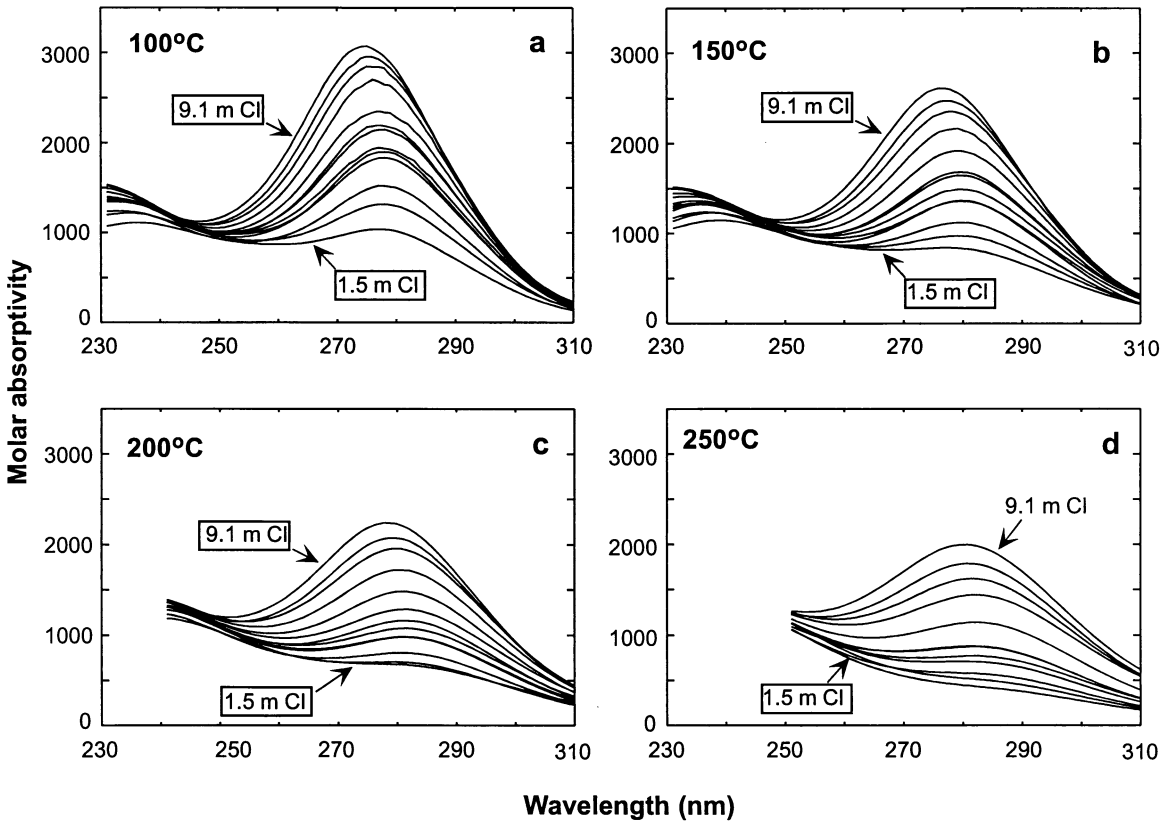

Fig. 3. Apparent molar absorptivity spectra of copper-bearing solutions: (a) 100 °C; (b) 150 °C; (c) 200 °C; and (d) 250 °C. The LiCl concentrations range from 1.5 m to 9.1 m and are listed in Table 1.

°C). Second, the molar absorptivity decreases with increasing temperature. This decrease in intensity coupled with an increase in baseline absorption (Fig. 2a) makes the data less accurate at 250 °C (see quantitative interpretation section below).

Figure 3 shows the apparent molar absorptivity spectra measured at 100 °C to 250 °C, and Figure 4 shows the dependence of molar absorptivities on chloride concentrations at two wavelengths for 150 °C spectra. At a given temperature, the intensity of the absorption band at approximately 270–280 nm increases systematically with increasing LiCl concentration (Fig. 3; Fig. 4), as does the shoulder at approximately 235–245 nm. The latter, however, reaches a plateau at 6 m LiCl and remains constant in the 6–9 m LiCl concentration range (Fig. 4). All previous room temperature studies have concluded that the major peak represents the absorption band of $CuCl_3^{2-}$ and that the shoulder is due to the absorption peak of $CuCl_2^-$ (Sugasaka and Fujii, 1976; Davis et al., 1978; Sharma and Millero, 1990). Another important feature of the spectra is that the absorption maximum shifts to lower wavelength as the LiCl concentrations increase from 6 m to 9 m, which might be due to the presence of a third complex (probably $CuCl_4^{3-}$).

4. QUANTITATIVE INTERPRETATION

The data fitting procedure has been described in detail by Brugger et al. (2001), so only a brief description is given here.

The relation between absorbance (A) at any given wavelength and molar concentrations (M_i) of the ith absorbing species is described by the Beer–Lambert law,

$$A = l \sum_{i=1}^{n} M_i \varepsilon_i, \tag{2}$$

where ε_i refers to the molar absorptivity of the ith species, n is the number of absorbing species, and l is the sample path length of the optical cell. This equation can be rewritten with molal concentration (m_i), commonly used in the thermodynamic calculations, by introducing the molar to molal transfer factor f_s (Eqn. 1):

$$A = \frac{1}{f_s} l \sum_{i=1}^{n} m_i \varepsilon_i. \tag{3}$$

In order to consider absorption at more than one wavelength, the Beer–Lambert law can be written in a matrix form as

$$\mathbf{A} = \mathbf{C} * \mathbf{E}, \tag{4}$$

where **C** is the matrix of concentrations of the absorbing species (number of solutions × number of absorbing species), **E** is the matrix of molar absorptivity coefficients (number of absorbing species × number of sampled wavelengths), and **A** is

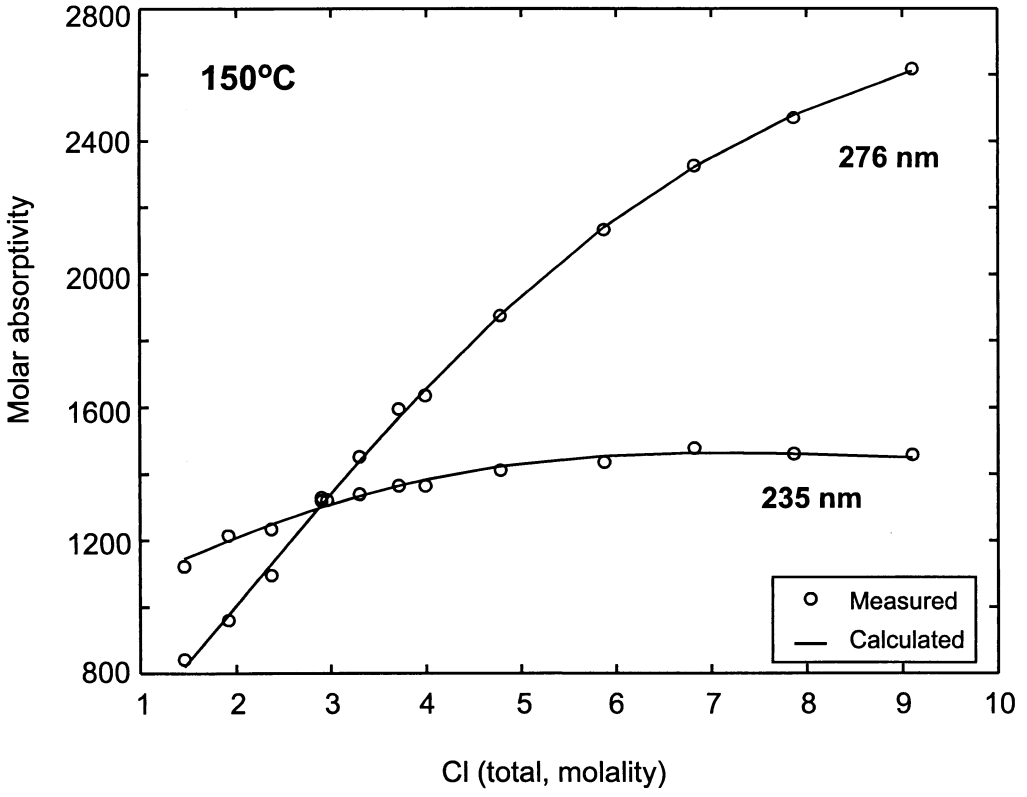

Fig. 4. Apparent molar absorptivity at 235 nm and 276 nm as a function of total chloride concentrations for copper-bearing solutions at 150 °C. The circles represent the measured molar absorptivities and the lines show the calculated values using the concentrations of copper–chloride complexes calculated using the log *K* values derived in this study (Table 4) and molar absorptivity spectra for copper–chloride complexes also derived in this study (Fig. 11).

the matrix of measured absorbances (number of solutions × number of sampled wavelengths). The goal of the quantitative interpretation of the spectroscopic data is to calculate the concentration and molar absorptivity coefficients of each absorbing species in each of the measured solutions, i.e., to find the matrices **C** and **E** that best reproduce the matrix **A**. This could be interpreted as a simple linear algebra problem; however, there is an infinite number of solutions that can be derived from linear algebra, whereas there is only one physically correct solution (e.g., Tauler and Casassas, 1989; Brugger et al., 2001). In general, physical constraints need to be applied in order to obtain a physically correct solution. Constraints that do not require any assumption on the chemistry of the system, except the number of different absorbing complexes present, include non-negativity (concentrations of species and molar absorptivity coefficients cannot be negative), closure (the sum of the concentrations of all the species containing a particular element is equal to the total known concentration of the element), and unimodality (only one maximum in the concentration profile) (e.g., Tauler and Casassas, 1989; Tauler and Casassas, 1992; De Juan et al., 1997). This type of analysis is called "model-free analysis" to distinguish it from the more complex data analysis that requires a thermodynamic model (e.g., Brugger et al., 2001). The thermodynamic model incorporates mass action, mass balance, and charge balance equations, as well as estimates of activity coefficients, that allows the calculation of a distribution of species for each experiment. Formation constants of each of the identified complexes are then fitted to the experimental data.

Data analysis in this study is developed in steps, by successively adding more constraints at each step and using the results of the previous, simpler steps as input for the next steps. In the first step, principal component analysis is used to estimate the number of absorbing species present in the experiments. In the second step, "Model-free" analysis is used to check the number of absorbing species, estimate the change in speciation with increasing ligand concentration, and give preliminary information about the shape of the molar absorptivity spectra for each of the absorbing species. This information is then used in the third step, where we incorporate a thermodynamic model and fit formation constants for each of the complexes. The 80 data points (231–310 nm) per spectrum were used at 100 °C and 150 °C for interpretation, and 70 data points (241–310 nm and 251–320 nm) were used at 200 °C and 250 °C. The fewer points at higher temperatures are due to the redshift of blank LiCl solutions with increasing temperature (Fig. 2).

4.1. Principal Component Analysis (PCA)

Principal component analysis (e.g., Malinowski and Howery, 1980) was used to provide information about the number of mathematical factors needed to describe the measured spectra.

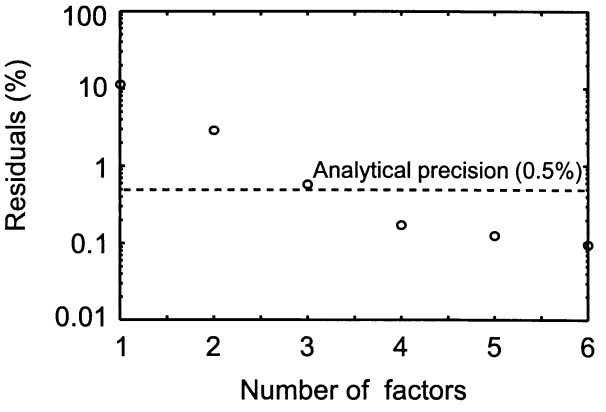

Fig. 5. Results of principal component analysis of apparent molar absorptivity data at 150 °C. The circles represent calculated residuals (R) corresponding to the number of factors on the x axis. The dashed line represents the estimated analytical uncertainty of 0.5%.

The residual function (R) in percentage used in the calculation is defined as

$$R = 100 \sqrt{\frac{\sum (x_i - x)^2}{\sum x_i^2}}, \qquad (5)$$

where x_i and x stand for the measured and calculated absorbance values, respectively. PCA of the spectra collected at each temperature indicates that at least three factors are needed to describe the spectra, corresponding to three Cu(I)–chloride complexes, e.g., at 150 °C (Fig. 5). We cannot determine if more factors are necessary, purely from the PCA, because the calculated residual percentage for four or more factors is less than our analytical precision of 0.5% (Fig. 5).

4.2. Model-Free Analysis

The "model-free analysis" was accomplished with the computer code described and made available by De Juan and Tauler (1999). We applied non-negativity constraints on the concentrations and molar absorptivity coefficients, as well as closure for Cu (i.e., sum of the concentrations of absorbing Cu complexes = total amount of copper in the solution). A unimodality constraint was applied, in order to avoid the first complex reappearing in the model at high LiCl concentrations, but even then the first complex was predicted to represent approximately 10% of the total copper concentration at the highest LiCl concentration in our experiments. This is a numerical artifact of the model and illustrates the difficulty in dealing with boundary conditions in these types of problems. Nevertheless, the results of the model-free analysis conducted with three complexes show that the species concentrations vary in a way expected for complexes arising from stepwise addition of ligands, i.e., the first complex is replaced by the second, which in turn is replaced by the third complex (Fig. 6a). The molar absorptivity spectra are smooth, with values in the range expected for charge-transfer spectra (Fig. 6b). The same analysis conducted with four complexes leads to molar absorptivity spectra for two species (number 2 and 3) that are very similar. The concentration profiles are not smooth, and those of species 2 and 3 are highly negatively correlated. This strongly suggests that we do not need more than three complexes to account for the measured spectra.

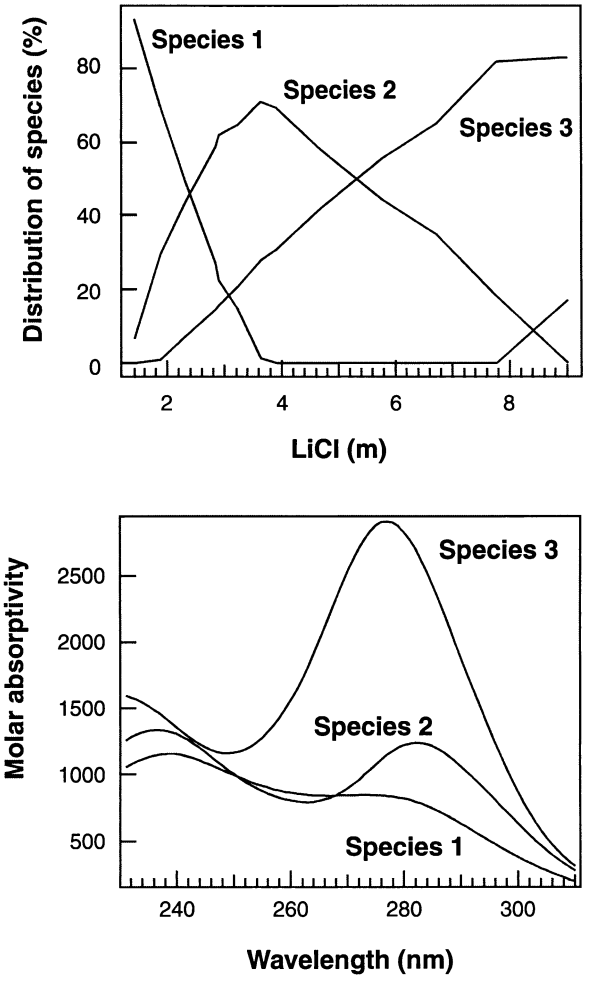

Fig. 6. Results of the "model-free" analysis of UV spectral data at 150 °C: (a) Distribution of three individual species as a function of LiCl concentration; (b) spectra of the three individual species.

4.3. Fitting Formation Constants for Copper(I) Chloride Complexes

A thermodynamic model is necessary to calculate the activities and concentrations of all the aqueous species present in the experimental solutions, and to fit equilibrium constants to the experimental data. The standard states used in this study are defined as the pure liquid at the temperature and pressure of interest for H_2O, and a hypothetically ideal one molal solution referenced to infinite dilution at the temperature and pressure of interest. The following aqueous species were considered in the model and calculations: Cl^-, Li^+, H^+, $LiCl_{(aq)}$, $HCl_{(aq)}$, Cu^+, and copper(I)–chloride complexes. As recommended by Brugger et al. (2001) and Liu et al. (2001), hydroxide species were not included in the model because of the acidic pH of the sample solutions and H_2O was not included because we do not consider waters of hydration for the copper complexes. Possi-

ble HCl_2^-, $LiCl_2^-$, and polynuclear complexes of LiCl and HCl were also not included in the model because of the lack of experimental data and thermodynamic properties, as discussed in Brugger et al. (2001). The concentrations and activities of the aqueous species were calculated by solving simultaneously the mass action equations (6–8), the mass balance equations (9–11), and a charge balance equation (12),

$$K_{HCl_{(aq)}} = \frac{m_{HCl_{(aq)}}\bar{\gamma}_{HCl_{(aq)}}}{m_{H^+}m_{Cl^-}\bar{\gamma}_{H^+}\bar{\gamma}_{Cl^-}}, \quad (6)$$

$$K_{LiCl_{(aq)}} = \frac{m_{LiCl_{(aq)}}\bar{\gamma}_{LiCl_{(aq)}}}{m_{Li^+}m_{Cl^-}\bar{\gamma}_{Li^+}\bar{\gamma}_{Cl^-}}, \quad (7)$$

$$K_{CuCl_i^{1-i}} = \frac{m_{CuCl_i^{1-i}}\bar{\gamma}_{CuCl_i^{1-i}}}{m_{Cu^+}\bar{\gamma}_{Cu^+}(m_{Cl^-}\bar{\gamma}_{Cl^-})^i}, \quad (8)$$

$$m_{Cu_{total}} = \sum_i m_{CuCl_i^{1-i}}, \quad (9)$$

$$m_{Cl_{total}} = m_{HCl_{(aq)}} + m_{LiCl_{(aq)}} + m_{Cl^-} + \sum_i i m_{CuCl_i^{1-i}}, \quad (10)$$

$$m_{Li_{total}} = m_{LiCl_{(aq)}} + m_{Li^+}, \quad (11)$$

$$m_{Li^+} + m_{Cu^+} + m_{H^+} = m_{Cl^-} + \sum_i [(1-i)m_{CuCl_i^{1-i}}], \quad (12)$$

m and $\bar{\gamma}$ represent the molal concentration and activity coefficients for the subscripted individual species, respectively, and i in Eqns. 8–10 and 12 indicates the number of the chloride ligands.

Activity coefficients of all aqueous species have to be estimated in order to relate activities and concentrations of those species. Our experiments necessarily cover a wide range of LiCl concentration and temperature and we need to describe the activity coefficients for both the main salt and trace concentrations of Cu complexes, making it difficult to choose a reliable way to calculate activity coefficients. We choose to use an extended form of the *b*-dot equation (Helgeson, 1969) because it was successfully used by Brugger et al. (2001) in fitting the mean molal stoichiometric activity coefficients for LiCl solutions and Cu(II)–chloride complexes at LiCl concentrations up to 18 m and temperatures up to 90 °C [see Fig. 5 in Brugger et al. (2001) and the related discussion in their paper]. Following Brugger et al. (2001) we use the following equation to estimate individual ionic activity coefficients ($\bar{\gamma}_n$) for charged species:

$$\log(\bar{\gamma}_n) = -\frac{A_\gamma Z_n^2 \bar{I}^{1/2}}{1 + B_\gamma \mathring{a}_n \bar{I}^{1/2}} + b_{\gamma,LiCl}\bar{I} + b_{\gamma_{sq},LiCl}\bar{I}^2 + \Gamma_\gamma, \quad (13)$$

where A_γ and B_γ are the Debye–Hückel solvent parameters taken from Helgeson and Kirkham (1974), and $b_{\gamma,LiCl}$ is the extended-term parameter (*b*-dot coefficient) for LiCl-dominated solutions, $\mathring{a}_n$ is the distance of closest approach for ion n, and is given a value of 5 Å for divalent and trivalent ions, and 4.0 Å for monovalent ions, except for H^+ which was given a value of 9 Å (e.g., Kielland, 1937). $\bar{I}$ is the effective ionic strength on the molal scale of concentration. Γ_γ is a mole fraction to molality conversion factor and $b_{\gamma_{sq}}$,LiCl is a quadratic term added to extend the *b*-dot equation to high chloride concentration (up to 18 molal LiCl) solutions (Brugger et al., 2001). This approach allows us to describe accurately the available mean molal stoichiometric activity coefficient data for LiCl solutions (i.e., Holmes and Mesmer, 1983), and use the same function to describe the activity coefficients for copper chloride complexes.

Table 3. The b-dot parameter ($b_{\gamma,LiCl}$), Setchénow coefficient ($b_{\gamma,LiCl_{(aq)}}$), and the extended quadratic coefficient ($b_{\gamma_{sq}}$,LiCl) used in activity coefficient calculations. The formation constants for $LiCl_{(aq)}$ and $HCl_{(aq)}$ calculated using SUPCRT92 (Johnson et al., 1992) are also given.

T (°C)	$b_{\gamma,LiCl}$ (m^{-1})	$b_{\gamma,LiCl_{(aq)}}$ (m^{-1})	$b_{\gamma_{sq}}$,LiCl $\times 10^3$ (m^{-2})	log $K_{LiCl_{(aq)}}$	log $K_{HCl_{(aq)}}$
100	0.108	0.336	1.18	−1.181	−0.748
150	0.094	0.300	0.174	−0.874	−0.517
200	0.069	0.325	0.184	−0.500	−0.142
250	0.043	0.377	0.201	−0.033	−0.389

The activity coefficient for the neutral species, $LiCl_{(aq)}$, was estimated with the Setchénow equation (Setchénow, 1889; see Brugger et al., 2001)

$$\log(\bar{\gamma}_{LiCl_{(sq)}}) = b_{\gamma,LiCl_{(sq)}}\bar{I} + \Gamma_\gamma. \quad (14)$$

Values of the *b*-dot coefficient ($b_{\gamma,LiCl}$), Setchénow coefficient ($b_{\gamma,LiCl_{(aq)}}$) and the extended quadratic coefficient ($b_{\gamma_{sq}}$,LiCl) at each experimental temperature were fitted to experimental values of the mean stoichiometric molal activity coefficients for LiCl (Holmes and Mesmer, 1983) following the procedure of Pokrovskii and Helgeson (1997) and Brugger et al. (2001) and are listed in Table 3. Figure 7 shows that the extended *b*-dot model accurately reproduces the experimental values of the mean stoichiometric molal activity coefficient of LiCl over the range of concentrations used in our experiments.

Activity coefficients of the two other neutral species, $HCl_{(aq)}$ and $CuCl_{(aq)}$, were assumed to be unity because they are only minor species in the solutions and acid concentrations are not required in our data interpretation.

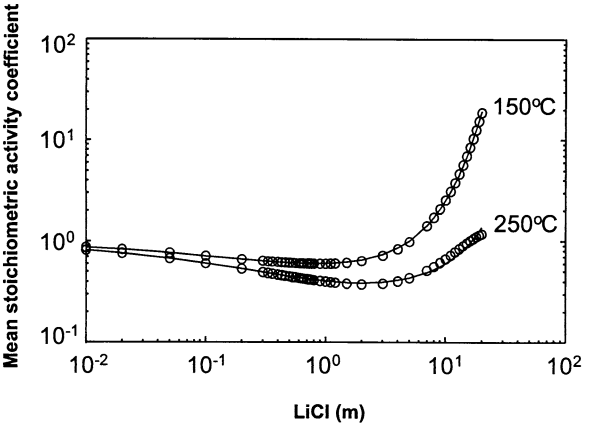

Fig. 7. The mean stoichiometric molal activity coefficients of LiCl. The circles represent the values calculated using Pitzer parameters fitted by Holmes and Mesmer (1983). The lines show predicted values using parameters and b-dot extension derived in this study.

Table 4. Logarithm of formation constants for copper(I)–chloride complexes derived from UV spectrophotometric experiments. The uncertainty ranges are shown in the parentheses.

	log *K*			
Reactions	100 °C	150 °C	200 °C	250 °C
$Cu^+ + 2Cl^- = CuCl_2^-$	4.84 (−0.13/+0.27)	5.13 (−0.2/+0.2)	5.27 (−0.5/+0.5)	5.93 (−0.6/+0.8)
$Cu^+ + 3Cl^- = CuCl_3^{2-}$	3.91 (−0.15/+0.15)	3.86 (−0.2/+0.15)	3.55 (−0.5/+0.5)	3.81 (−0.4/+0.7)
$Cu^+ + 4Cl^- = CuCl_4^{3-}$	1.3 (−0.6/+0.4)	1.26 (−0.8/+0.5)	1.27 (−0.9/+0.5)	1.59 (−0.9/+0.6)

4.3.1. Choice of speciation model

The quantitative analysis requires an assumption about the number and stoichiometry of the absorbing copper complexes present in the experimental solutions. The PCA and the model-free analysis of spectra indicated that three complexes are needed to describe the experimental absorbance spectra. Previous room-temperature UV spectral studies have concluded that two complexes, namely $CuCl_2^-$ and $CuCl_3^{2-}$, are predominant in solutions with chloride concentrations below 6 m. Two recent independent solubility studies (Liu et al., 2001; Xiao et al., 1998) agreed that $CuCl_{(aq)}$ predominates at chloride concentrations between 0.01–0.1 m and $CuCl_2^-$ predominates at chloride concentrations between 0.1 and 2 m at temperatures from 25 °C to 300 °C. A recent EXAFS study of copper(I)–chloride complexes also suggests that $CuCl_2^-$ is predominant in solutions containing 0.2–0.4 m Cu and 0.5–2 m NaCl from 100 °C to 325 °C (Fulton et al., 2000a). Two room-temperature studies suggest the existence of $CuCl_4^{3-}$ in solutions with chloride concentration as low as 3 M (Hikita et al., 1973; Ciavatta and Iuliano, 1998).

Polynuclear copper complexes such as $Cu_2Cl_4^{2-}$, suggested by Ahrland and Rawsthorne (1970) and Fritz (1980), were not included in our speciation model, because of the low copper concentrations (11–25 ppm) and high Cl/Cu mole ratio (6000 to 30,000) used in our study. Additionally, the UV spectra studies by Sharma and Millero (1990) showed that the apparent molar absorptivity of the copper–NaCl solutions is independent of copper concentration in the range from 50 to 200 μM. This indicates that no polynuclear complexes were formed under their experimental conditions. Furthermore, Fulton et al. (2000a) did not detect polynuclear copper–chloride species in their EXAFS study, conducted at much higher copper concentration (0.4 m) and lower Cl/Cu ratios (6) than in our experiments. Finally, we included a possible polynuclear species, $Cu_2Cl_4^{2-}$, in initial models and found that the resulting molar absorptivity spectra were unrealistic and the residuals were larger than in models without this species.

Several alternative speciation models were considered in preliminary fits. Two models containing only two mononuclear species (either $CuCl_2^-$ and $CuCl_3^{2-}$ in one case, or $CuCl_3^{2-}$ and $CuCl_4^{3-}$ in another), generated very large relative residuals ($\gg$1%) and resulted in unrealistic molar absorptivity spectra. A five-species model (including $CuCl_5^{4-}$) reduced the relative residual (Fig. 5), but generated unrealistic molar absorptivity spectra, e.g., the molar absorptivities of one complex become extremely high while molar absorptivities of other species decrease substantially.

Based on the preliminary fits, we choose to include $CuCl_{(aq)}$, $CuCl_2^-$, $CuCl_3^{2-}$, and $CuCl_4^{3-}$ in our final speciation model. We included $CuCl_{(aq)}$ species in the speciation model because its presence may affect the calculated concentrations of other copper complexes, especially at the lower LiCl concentrations in our experiments (i.e., less than 2 m LiCl). Although $CuCl_{(aq)}$ was included in the speciation model, its absorbance is negligible and ignored for two reasons. First, according to the results of solubility studies of Liu et al. (2001) and Xiao et al. (1998) $CuCl_{(aq)}$ is only a minor species under the experimental conditions of this study, i.e., $<$5 mol % of total copper at the lowest chloride concentration of 1.5 molal and much less than 1 mol % at higher chloride concentrations. Second, the molar absorptivity of $CuCl_{(aq)}$ is expected to be low, because it has a linear coordination structure similar to $CuCl_2^-$ (i.e., H_2O–Cu-$Cl_{(aq)}$ and $CuCl_2^-$; Fulton et al., 2000a) and we found the molar absorptivity of $CuCl_2^-$ to be low in our interpretation. The log *K* of formation values for $CuCl_{(aq)}$ were fixed to those from Liu et al. (2001). The molar absorptivities and log *K* values for the three complexes ($CuCl_2^-$, $CuCl_3^{2-}$, and $CuCl_4^{3-}$) were optimized simultaneously according to the procedure described below.

4.3.2. Calculation of formation constants for copper(I)–chloride complexes

The calculation of formation constants for copper(I)–chloride complexes includes two optimization algorithms performed in an outer and inner programming loop. In the inner loop, the distribution of species was calculated for a given set of formation constants (log *K*) for the copper(I)–chloride complexes, and the molar absorptivity of each unknown absorbing species was optimized with a quadratic programming method (Nemaier, 1998). In the outer loop, the log *K* values are varied using a simplex algorithm (Nelder and Mead, 1965) until a local minimum for the residual function is obtained. The residual function used in the calculation is defined as the sum of the squares of the difference between measured and calculated absorbances.

The formation constants for copper(I)–chloride complexes derived from this study are listed in Table 4. The uncertainties in the derived log *K* values shown in Table 4 are discussed in the following section.

4.4. Estimation of Uncertainties

Accurate estimation of the total uncertainties in derived log *K* values is difficult due to the unknown uncertainties in indi-

vidual aspects of our interpretation, such as experimental error, accuracy of the activity coefficients, and colinearity of both concentrations and molar absorptivities for each species, although we discuss the effects of some of these below.

In order to estimate uncertainties in the fitted formation constants, we calculated residual maps at each temperature as a function of the formation constants for $CuCl_2^-$, $CuCl_3^{2-}$, and $CuCl_4^{3-}$, as described by Brugger et al. (2001) and Liu et al. (2001). Two-dimensional sections through the three-dimensional (3D) residual space are used to study the nature of the minimum (i.e., local or unique) and estimate the magnitude of the uncertainty in the derived formation constants. Figure 8a and b shows two examples of residual maps for 150 °C experiments: log $K_{CuCl_2^-}$ versus log $K_{CuCl_3^{2-}}$ and log $K_{CuCl_3^{2-}}$ versus log $K_{CuCl_4^{3-}}$. The residual values shown in the maps have been normalized to relative residuals R as defined by Eqn. 5. There is a single minimum in both maps, which indicates all three species were present in detectable concentrations in the experimental solutions at 150 °C. An approximate confidence region, defined by the contour of 1.53% at the 90% confidence level, was estimated using a statistical method for nonlinear regression (Draper and Smith, 1998, p. 516). The uncertainty in each log K value was approximated by the range of the 90% confidence contour at the given optimized log K values for the other two complexes, e.g., the uncertainty is $-0.2/+0.2$ for $CuCl_2^-$ (Fig. 8a), $-0.2/+0.15$ for $CuCl_3^{2-}$ (Fig. 8a, b), and $-0.8/+0.5$ for $CuCl_4^{3-}$ at 150 °C (Fig. 8b).

In order to evaluate the effects of experimental uncertainties on the derived log K values, a synthetic absorbance data set was generated by adding normally distributed errors to the copper and LiCl concentrations and the fitted spectra. Then, residuals between the fitted and synthetic spectra were calculated as functions of log K values for copper(I)–chloride complexes. The residual maps calculated for the synthetic absorbance data at 150 °C, where we assumed random errors of 2% in the LiCl and Cu concentrations and 0.002 units in absorbance, are similar to the maps calculated for the experimental data (i.e., Fig. 8), and do not change the magnitude of the uncertainties on the log K values. This suggests that the large uncertainty of log K values defined by a 90% confidence region is an inherent characteristic of the spectrophotometric method.

The 90% confidence contour in the residual map for the 250 °C experiments shows an open end with respect to $CuCl_3^{2-}$ (Fig. 9) due to the low concentration of this complex (less than 20 mol %) in these experiments. However, a minor change of log $K_{CuCl_3^{2-}}$ results in considerable change in the molar absorptivity spectra of $CuCl_3^{2-}$ and $CuCl_4^{3-}$, as indicated by the dashed lines that represent the ratio of maximum molar absorptivity of $CuCl_3^{2-}$ and $CuCl_4^{3-}$ (Fig. 9). For example, an increase of $K_{CuCl_3^{2-}}$ by 0.5 log units would result in a maximum molar absorptivity of $CuCl_3^{2-}$ of 9250 while that of $CuCl_4^{3-}$ would be 2200, which is unrealistic based on the nature of molar spectra of these species at other temperatures. Therefore, an additional constraint on the ratio of molar absorptivity spectra was used to determine the uncertainty in log $K_{CuCl_3^{2-}}$. A value of 5 for the ratio of maximum molar absorptivity of $CuCl_3^{2-}$ and $CuCl_4^{3-}$ was chosen to define the upper uncertainty in log K for $CuCl_3^{2-}$ (Fig. 9).

The most difficult aspect of our interpretation is to quantify the uncertainties in log K values resulting from the activity coefficient model. The activity coefficients for $LiCl_{(aq)}$, Li^+, and Cl^- are fitted to experimental data for the mean molal stoichiometric activity coefficients of LiCl, which are important in calculating the effective ionic strength in LiCl solutions. We cannot assess the accuracy of those activity coefficients, however, because of unknown uncertainties in the formation constant for $LiCl_{(aq)}$ and the Setchénow coefficient for $LiCl_{(aq)}$. The individual activity coefficients for the copper–chloride complexes depend on the parameters in Eqns. 13 and 14: A, B_γ, $\mathring{a}_n$ $b_{\gamma,LiCl}$, $b_{\gamma,sq,LiCl}$, and the effective ionic strength $\bar{I}$. Except for $\mathring{a}_n$, all of the parameters are well known or fitted to experimental data for LiCl, so we focus on the effects of the uncertainties in the ion size parameter ($\mathring{a}_n$) on the derived log K values. The calculated activity coefficients, especially for $CuCl_4^{3-}$, are sensitive to the choice of the $\mathring{a}_n$ (Fig. 10). For example, the log activity coefficient of $CuCl_4^{3-}$ in a 1.5 m LiCl solution at 250 °C calculated using $\mathring{a}_n = 4$ is approximately 0.5 log unit lower than the value using $\mathring{a}_n = 5$, and this discrepancy increases with increasing chloride concentration (Fig. 10). However, the fitted log K values using $\mathring{a}_n = 4$ for $CuCl_3^{2-}$ and $CuCl_4^{3-}$ are only 0.05 and 0.5 log units lower than the values using $\mathring{a}_n = 5$, respectively. This difference is within the uncertainties estimated from the residual maps (Table 4). Either we need an independent method to determine the magnitude of the $\mathring{a}_n$ parameters or alternative activity coefficient models, both of which are beyond the scope of our study.

In summary, it is difficult to quantify accurately the uncertainties in our fitted log K values because there are too many unknowns. However, we have demonstrated that the variability in fitted log K values, resulting from some differences in our assumptions about experimental error and the activity coefficient model, is probably within our estimated uncertainties. We note that the calculated molar absorbance spectra for copper complexes and their calculated concentrations of species in our experiments agree qualitatively with the results of our model-free analysis (see below). This suggests that even though our thermodynamic model, especially the activity coefficient estimates, is uncertain, our interpretation and estimates of activity coefficients are reasonable. This conclusion is further supported by the fact that the stability constants gained in this study in LiCl solutions compare well with stability constants obtained in other studies in different salts (see below).

4.5. Calculated spectra

The calculated molar absorptivity spectra of individual copper(I)–chloride complexes are shown in Figure 11. The peak position and shapes of molar absorptivity spectra for $CuCl_2^-$ and $CuCl_3^{2-}$ complexes are in a good agreement with previous room temperature spectral studies (Hikita et al., 1973; Davis et al., 1978; Sharma and Millero, 1990). The $CuCl_2^-$ complex displays only an absorption shoulder at 230–240 nm with relatively low molar absorbance of ~1100. This shoulder disappears under the chloride-to-water charge-transfer band of LiCl as temperature increases. $CuCl_3^{2-}$ has a main absorption peak around 270–290 nm and a lower intensity band at wavelengths below 235 nm. Our calculations also clearly indicate that a new complex, probably $CuCl_4^{3-}$, is required to describe the spectra. The increase of the $CuCl_4^{3-}/CuCl_3^{2-}$ ratio with

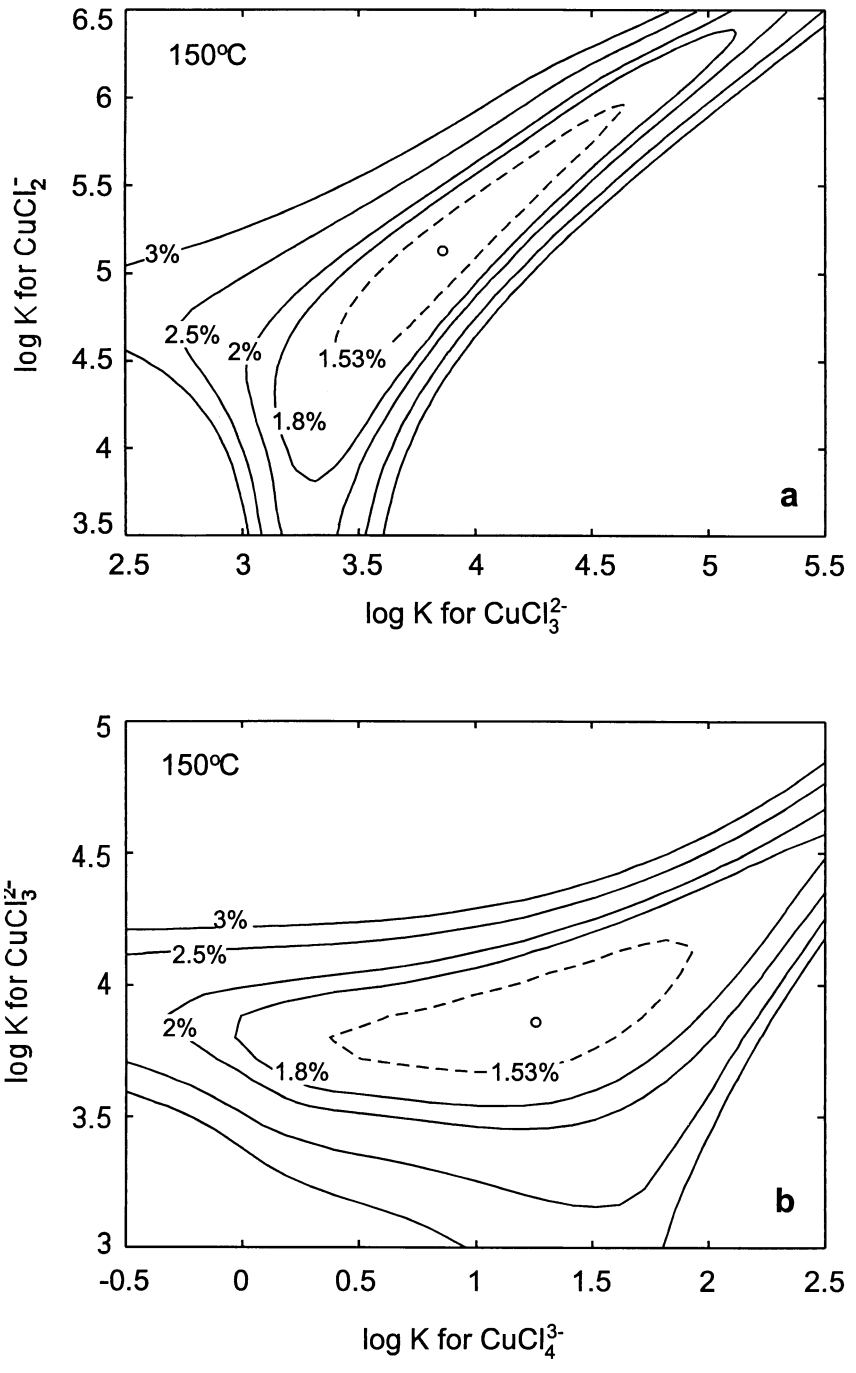

Fig. 8. Residual maps for copper–chloride complexing experiments at 150 °C. The solid lines and labeled values represent the residuals (R) between the measured and calculated absorbance spectra as a function of log K values of formation constants for copper(I)–chloride complexes. The dashed line represents a 90% confidence region. The circles show the fitted log K values. (a) $CuCl_2^-$ vs. $CuCl_3^{2-}$; (b) $CuCl_3^{2-}$ vs. $CuCl_4^{3-}$.

increasing chloride concentration is responsible for the shifting of the 275 nm peak of measured spectra towards lower wavelength, as mentioned in the qualitative interpretation section.

As temperature increases, the peak positions of $CuCl_3^{2-}$ and $CuCl_4^{3-}$ shift by several nanometers towards lower energy (Fig. 12). This redshift is characteristic of charge-transfer-to-solvent (CTTS) spectra (Blandamer and Fox, 1970; Davis et al., 1978).

Figure 13 shows the quality of the fit for three 150 °C solutions with different chloride concentrations together with the contribution of each absorbing species to the total absorbance. The absorption band at 270–290 nm is due primarily to $CuCl_3^{2-}$, and the band at 230–250 nm is due mainly to $CuCl_2^-$ with a minor contribution from $CuCl_3^{2-}$ for 1.5 m LiCl solution (Fig. 13a). For a solution with 4.8 m LiCl, the 270–290 nm

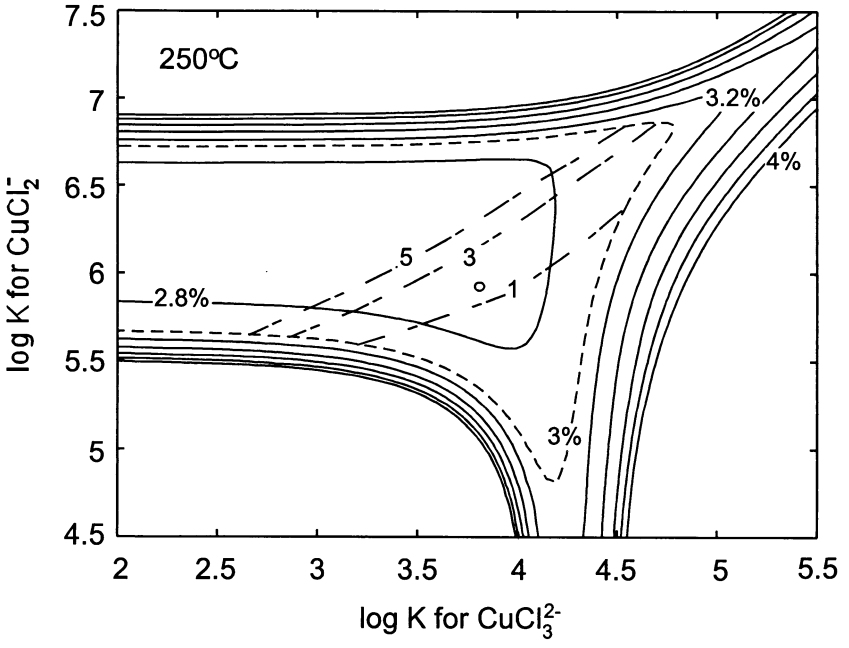

Fig. 9. Residual map for copper–chloride complexing experiments at 250 °C. Solid and dashed lines as for Fig. 8. The dashed–dotted lines show the ratio of calculated maximum molar absorptivity of $CuCl_3^{2-}$ (289 nm) to $CuCl_4^{3-}$ (278 nm) ($\varepsilon_{max,CuCl_3^{2-}}/\varepsilon_{max,CuCl_4^{3-}}$).

absorption band results from the combination of $CuCl_3^{2-}$ and $CuCl_4^{3-}$ (Fig. 13b). For a solution with 9.1 m LiCl, there is almost no contribution of $CuCl_2^-$ to the spectrum, and the absorption bands are mainly due to $CuCl_4^{3-}$ plus a minor contribution of $CuCl_3^{2-}$ (Fig. 13c). With increasing chloride concentration, the intensity of the absorption band at 270–290

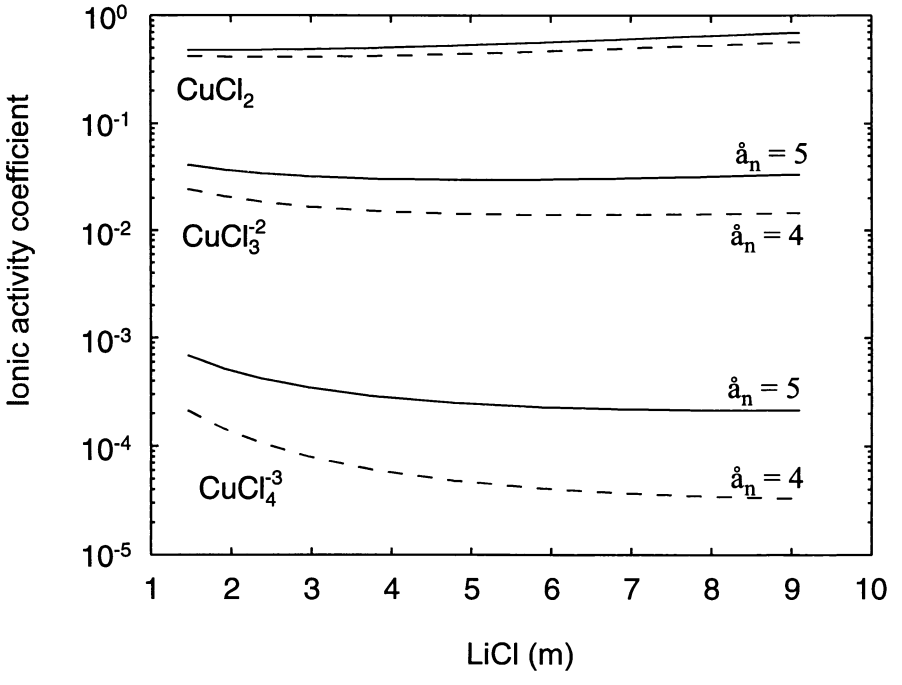

Fig. 10. Calculated individual ionic activity coefficients for copper(I)–chloride complexes as a function of LiCl concentration at 250 °C. Solid lines represent the values using an ion size parameter ($å_n$) = 5 and dashed lines are for ($å_n$) = 4.

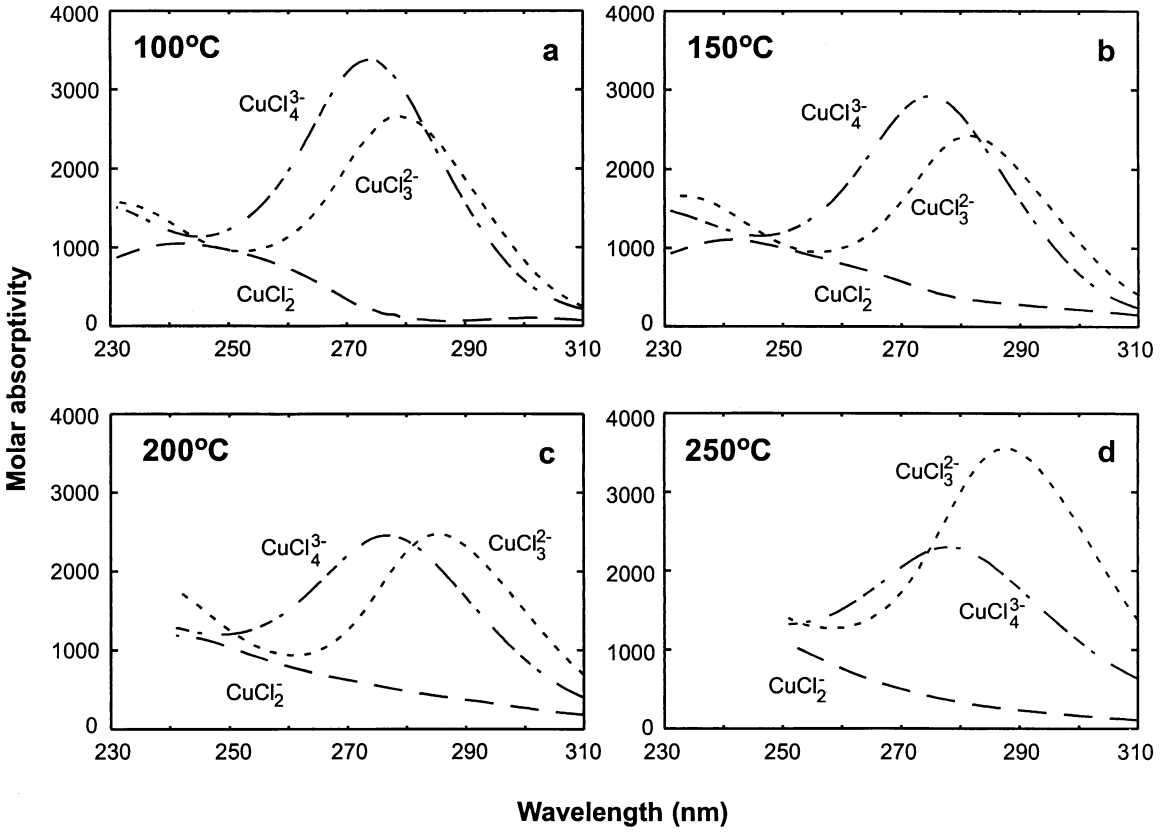

Fig. 11. Calculated molar absorptivity spectra of copper(I)–chloride complexes: (a) 100 °C; (b) 150 °C; (c) 200 °C; and (d) 250 °C.

nm increases relative to the absorption at around 230–250 nm. This is due to the decrease of $CuCl_2^-$ contribution and increase of $CuCl_3^{2-}$ and $CuCl_4^{3-}$ contributions (Fig. 13).

4.6. Speciation of copper(I) in acid LiCl solutions

Figure 14 shows the distribution of copper(I)–chloride complexes as a function of total chloride concentration in LiCl solutions based on the formation constants for copper(I)–chloride complexes derived in this study. At 100 °C, $CuCl_2^-$ contributes for about 60 mol % in the 1.5 m LiCl solutions and its concentration decreases gradually with increasing chloride concentrations (Fig. 14a). $CuCl_3^{2-}$ predominates in the 100 °C solutions with chloride concentration between 2 and 7 m, then $CuCl_4^{3-}$ becomes dominant. With increasing temperature to 250 °C, $CuCl_2^-$ increases in importance relative to $CuCl_3^{2-}$ at any chloride concentration. For example, at 100 °C $CuCl_3^{2-}$ represents more than 60 mol % of total copper and $CuCl_2^-$ represents only about 20 mol % in a 4 m LiCl solution [Fig. 14(a)], but at 250 °C $CuCl_2^-$ is about 70 mol % and $CuCl_3^{2-}$ is less than 20 mol % of the total copper concentration at the same LiCl concentration (Fig. 14d). This indicates that $CuCl_3^{2-}$ is more stable at lower temperatures. This study provides a more complete and accurate speciation of copper complexes than presented in Liu et al. (2001), because formation constants for $CuCl_3^{2-}$ could not be obtained under the conditions of temperature and total chloride concentrations used in their study.

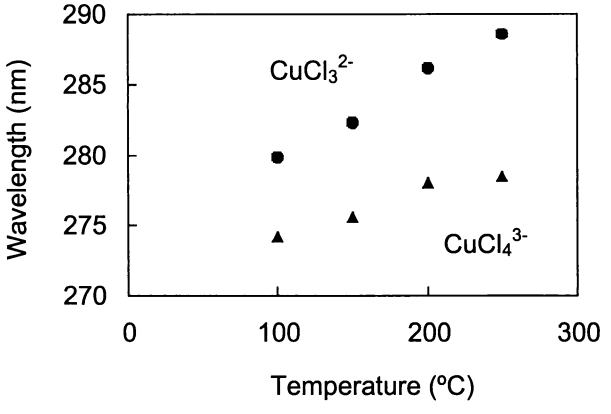

Fig. 12. The wavelength of the maximum molar absorptivities of $CuCl_3^{2-}$ (circles) and $CuCl_4^{3-}$ (triangles) as a function of temperature.

The UV spectra of copper(I)–chloride complexes can be used to understand the coordination structure of the complexes. According to ligand field theory, splitting of the degeneracy of $4p_{x,y,z}$ orbitals of free Cu(I) ion by a ligand field would lead to the structure of Cu(I) complexes changing from linear (for 2-coordination number) to trigonal planar or T-shaped (for 3-coordination number), and tetrahedral (for 4-coordination

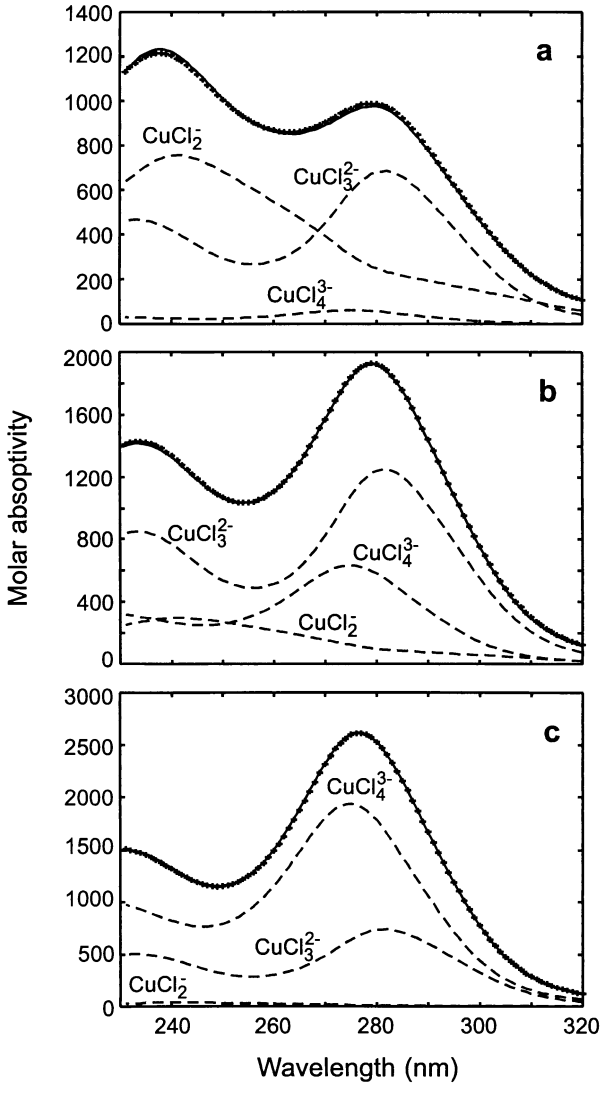

Fig. 13. Absorptivity spectra of copper(I)–chloride solutions and individual complexes (dashed lines) at 150 °C in (a) 1.9 m, (b) 4.9 m, and (c) 9.1 m LiCl solutions. The solid lines represent measured absorbance and are superimposed on crosses that are calculated using the results of this study.

number) (Kau et al., 1987). Recent EXAFS studies show that both $CuCl_{(aq)}$ and $CuCl_2^-$ display linear coordination in water up to 325 °C, and that there is no evidence of water of hydration in the first-coordination shell of $CuCl_2^-$ (Fulton et al., 2000a) and $CuBr_2^-$ complexes (Fulton et al., 2000b).

EXAFS studies of higher order Cu(I)–chloro complexes are not yet available. The addition of a chloride ion to the linear $CuCl_2^-$ complex must be accompanied by a change in the geometry of the complex. This change in geometry is reflected in the characteristic of the electronic spectrum of $CuCl_3^{2-}$, that differs strongly from the spectrum of $CuCl_2^-$ both in terms of absolute molar absorbance and position of the absorbance bands (Fig. 11). The molar absorbance spectrum for $CuCl_4^{3-}$ is similar to that of $CuCl_3^{2-}$, with a small redshift. Consequently, both $CuCl_4^{3-}$ and $CuCl_3^{2-}$ may possess a tetrahedral geometry. The complex $CuCl_4^{3-}$ is common in crystals, and is found in the only natural Cu(I)–chloride mineral, nantokite (Hull and Keen, 1994). Alternatively, the structure of $CuCl_3^{2-}$ could be trigonal planar as in Cu_2MnCl_4 (Pfitzner and Lutz, 1993) and in some other three-coordinate Cu(I) organic complexes (Kau et al., 1987).

5. DISCUSSION

5.1. Comparison with Previous Studies

Detailed discussion of previous studies of copper(I) complexes studies at high temperature is available in the recent paper on cuprite solubility by Liu et al. (2001) and will not be repeated here.

The formation constants derived in this study for the $CuCl_2^-$ complex are in good agreement with the recent solubility studies of Xiao et al. (1998) and Liu et al. (2001), except for the 250 °C value (Fig. 15a). Although still within quoted uncertainty, the disagreement at 250 °C is probably due to the lower accuracy of our experiments at this temperature. Also good agreement is obtained between those experimental values and isocoulombic estimates by Ruaya (1988) from 100 °C to 150 °C, but then deviate for higher temperatures (Fig. 15a). In contrast, the three sets of experimental results are in poor agreement with theoretical estimates by Sverjensky et al. (1997), probably due to the lack of experimental data at higher temperatures available at that time.

For $CuCl_3^{2-}$, there is poor agreement between the log K values of our study and experimental results of Xiao et al. (1998) (Fig. 15b). Their log $K_{CuCl_3^{2-}}$ results are likely to be incorrect because the maximum chloride concentration of their experiments was 1 m and the $CuCl_3^{2-}$ complex should not be detectable at this salt concentration at temperatures greater than 100 °C (Liu et al., 2001; this study). The log $K_{CuCl_3^{2-}}$ values of this study are within the upper limits (<5) estimated by Liu et al. (2001) at 150 °C and 250 °C, however. Our results are in excellent agreement with the theoretical estimates by Sverjensky et al. (1997). The disagreement between our results and the isocoulombic estimates of Ruaya (1988) is approximately 0.5–1 log units (Fig. 15b).

Experimental high-temperature log K values for $CuCl_4^{3-}$ are not available in the literature, though several room temperature experimental studies have already identified this complex and estimated its log K values. The values of Sukhova et al. (1968) (potentiometric study), Hikita et al. (1973) (solubility study), and Ciavatta and Iuliano (1998) (potentiometric study) are in poor agreement and 2–3 log units higher than our 100 °C values (Fig. 15c). The log K values for $CuCl_4^{3-}$ from these room temperature studies may not be reliable, because the maximum chloride concentration used in experiments of Hikita et al. (1973) and Ciavatta and Iuliano (1998) was 3 m, not high enough to detect $CuCl_4^{3-}$ unequivocally, and in the Sukhova et al. (1968) study they probably overfitted their data [i.e., they fitted formation constants for as many as 19 copper(I)–chloride complexes].

5.2. Smoothed log K Values for Copper(I)–Chloride Complexes

In order to provide equations for interpolation of log K values derived at different temperatures, the experimentally

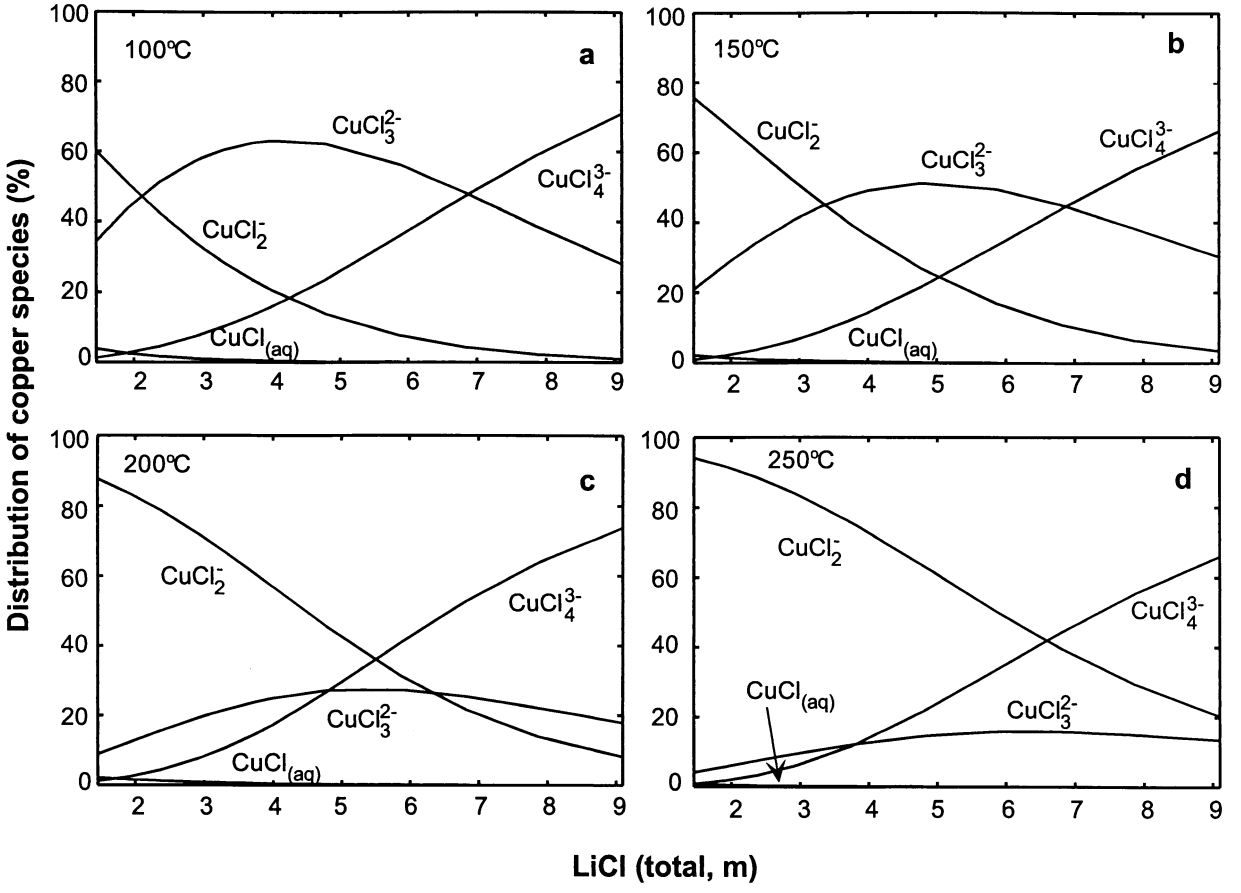

Fig. 14. Calculated distributions of copper(I)–chloride complexes as a function of chloride concentrations in the experimental LiCl solutions of this study: (a) 100 °C; (b) 150 °C; (c) 200 °C; and (d) 250 °C.

derived formation constants for copper(I) complexes from this study and several previous studies were fitted with the density model equation of Anderson et al. (1991) that is rewritten in the format of log K values for the formation reactions

$$\log K = -\frac{1}{2.303}\left[p_1 + \frac{p_2}{T} + \frac{p_3 \ln \rho_w}{T}\right], \qquad (15)$$

where ρ_w is density of pure water at temperature (T) in Kelvin, taken from Lemmon et al. (2000). p_1, p_2, and p_3 are constants characteristic of each chemical reaction, and were regressed from the experimental log K values for $CuCl_{(aq)}$, $CuCl_2^-$, $CuCl_3^{2-}$, and $CuCl_4^{3-}$.

For $CuCl_{(aq)}$, there is up to 0.5 log unit difference between the log K values from Liu et al. (2001) and Xiao et al. (1998). The log K values derived by Xiao et al. (1998) for copper(I)–chloride complexes at 200 °C–300 °C, and especially those for $CuCl_{(aq)}$, rely on the accuracy of the data for Ag–Cl complexes. Because there is some disagreement in the log $K_{AgCl_{(aq)}}$ values determined in the experimental studies of Seward (1976) and Zotov et al. (1986) at 200 °C–300 °C, we did not include the Xiao et al. (1998) values of log $K_{CuCl_{(aq)}}$. Three high-temperature log K data sets for $CuCl_2^-$ (Xiao et al., 1998; Liu et al., 2001; this study except for 250 °C value) are in good agreement and were included in the regression. The 25 °C data from Fritz (1980; for $CuCl_2^-$ and $CuCl_3^{2-}$) and Ciavatta and Iuliano (1998; for $CuCl_3^{2-}$ and $CuCl_4^{3-}$) were also included in the fitting.

The fitted density model parameters (p_1, p_2, and p_3 in Eqn. 15) are listed in Table 5. The calculated log K values for copper(I)–chloride complexes based on Eqn. 15 at selected temperatures are tabulated in Table 6 and plotted as a solid line in Figure 15. The density model equation (Eqn. 15) with parameters in Table 5 can be used to extrapolate log K for copper–chloride complexes to 350 °C and water vapor saturated pressure, based on good agreement between extrapolated values of log K and experimental values of Var'yash (1992) for $CuCl_2^-$ (Fig. 15a). Reliable extrapolations to higher temperatures and pressures awaits further study.

5.3. Geological Application

A number of thermodynamic modeling studies have been dedicated to copper transport in ore-forming systems, such as sediment-hosted copper deposits (Rose, 1976; Haynes, 1986; Haynes and Bloom, 1987a; Haynes and Bloom, 1987b; Sverjensky, 1987), modern seafloor hydrothermal systems (Seyfried and Ding, 1995; Xiao et al., 1998), and porphyry systems (e.g., Hezarkhani et al., 1999). However, some of these calculations were either limited to room temperature (e.g., Rose, 1976;

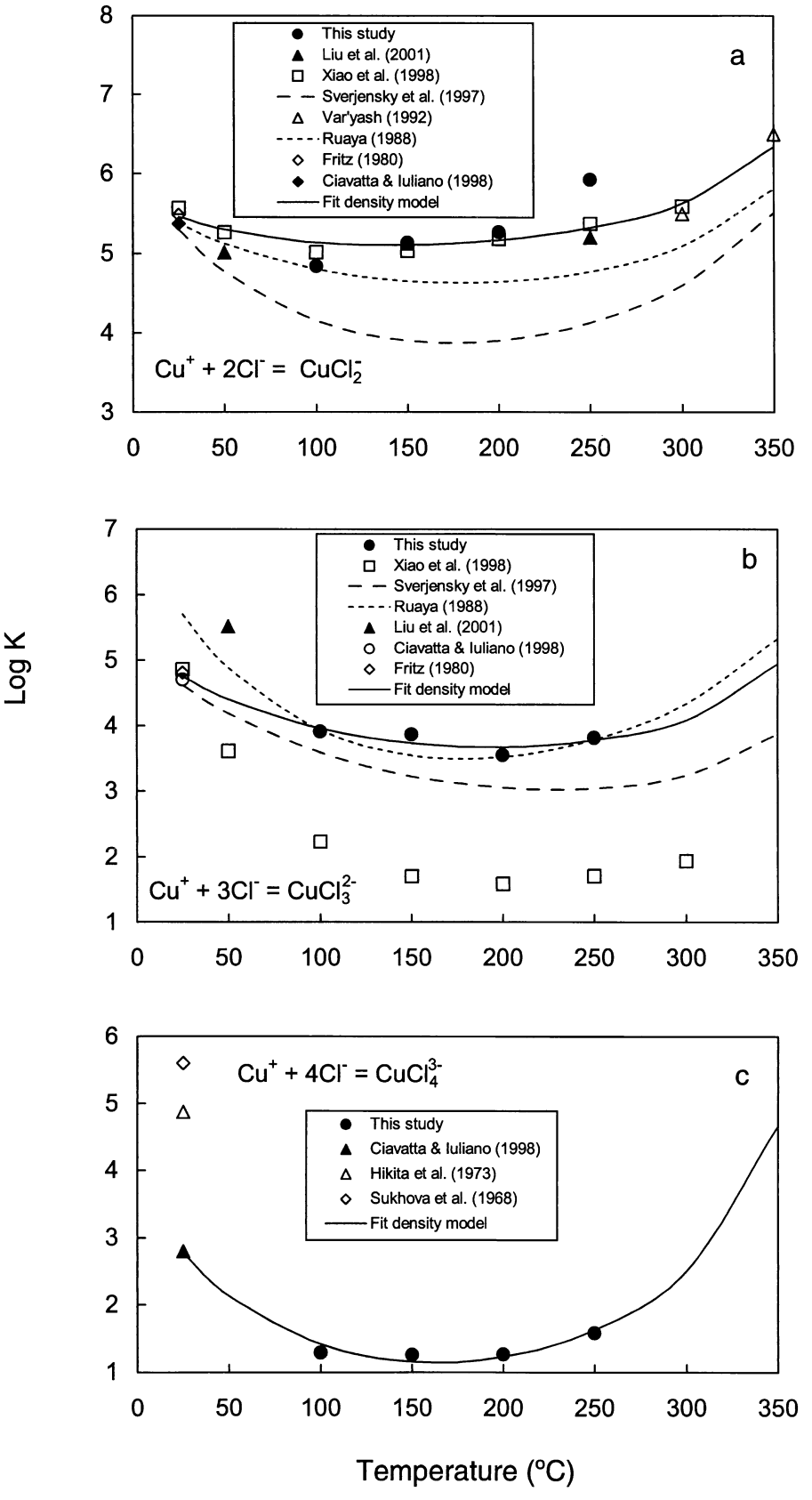

Fig. 15. Logarithms of the formation constants for (a) $CuCl_2^-$, (b) $CuCl_3^{2-}$, and (c) $CuCl_4^{3-}$ complexes as a function of temperature from 25 °C to 350 °C. Results from this study and selected previous studies are shown for comparison.

Table 5. Regressed parameters in the density model equation [Eqn. (15)] for copper(I)–chloride complexes.

	p_1	p_2	p_3	R^2
$CuCl_{(aq)}$	−1.9498	−2258.510	6701.646	1.000
$CuCl_2^-$	−5.3809	−2124.137	6538.330	0.922
$CuCl_3^{2-}$	2.7309	−4053.364	8541.388	0.985
$CuCl_4^{3-}$	19.7776	−7737.343	20 373.86	0.992

Haynes and Bloom, 1987a, 1987b) or contained only one copper(I)–chloride complex (e.g., Seyfried and Ding, 1995; Hezarkhani et al., 1999). In addition, the chloride concentrations used in most of the modeling studies were below 2 m, lower than the salinities of many hydrothermal ore-forming systems (Fig. 1). The results of this study provide a good basis for modeling copper transport in such natural systems.

To illustrate how the thermodynamic properties for copper(I)-chloride complexes can be used to understand copper transport in hydrothermal environments, we calculated the solubility of chalcopyrite in 1–5 m NaCl solutions at 200 °C–350 °C, using different formation constants for copper(I)–chloride complexes of Sverjensky et al. (1997), Xiao et al. (1998), and this study. The redox conditions and sulfur contents were buffered with hematite–magnetite–pyrite mineral assemblage and pH = 5. These conditions are close to the Eh–pH ranges defined by the mineral stability fields for a porphyry copper system (e.g., Crerar and Barnes, 1976; Beane and Titley, 1981; Hezarkhani et al., 1999). In our calculations, the other equilibrium constants needed were calculated from SUPCRT92 and the original database (Johnson et al., 1992), except for the log K values for copper(I)–hydrosulfide complexes, which are from Mountain and Seward (1999). Activity coefficients were calculated using the B-dot equation (Helgeson, 1969). Note that the copper concentration at high NaCl concentration (3–5 m) solutions may be less accurate due to the limitation of the activity coefficient model, but without more detailed knowledge we cannot evaluate the accuracy of the predictions. Calculated chalcopyrite solubility in 5 m NaCl solutions as a function of temperature is shown in Figure 16a. Chalcopyrite solubility calculated using the log K values from this study is higher than those calculated using the values of Xiao et al. (1998) and Sverjensky et al. (1997), especially at temperatures greater than 300 °C (Fig. 16a). Using the log K values of our study, the predicted total dissolved copper concentration is approximately 2700 ppm at 350 °C. Chalcopyrite solubility decreases sharply to 6 ppm at 300 °C (Fig. 16a), indicating that most copper would precipitate when temperature decreases to 300 °C from 350 °C. This is consistent with measured homogenization temperatures representing chalcopyrite precipitation for many porphyry copper deposits, such as in the Southwestern US (250 °C–350 °C, Beane and Titley, 1981) and the Sungan porphyry copper deposit in Iran (300 °C–400 °C, Hezarkhani and Williams-Jones, 1998; Hezarkhani et al., 1999).

Chalcopyrite solubility was also calculated as a function of chloride concentrations at a given temperature. An example for 300 °C is shown in Figure 16b. The predicted chalcopyrite solubility in 1 m NaCl solutions based on log K values from this study is similar to that based on values of Xiao et al. (1998) (Fig. 16a). The discrepancy becomes greater as chloride concentration increases (Fig. 16b). This is not surprising because the log $K_{CuCl_3^{2-}}$ of this study are higher than those reported by Xiao et al. (1998) (Fig. 16b) and a new copper(I)–chloride complex, $CuCl_4^{3-}$, was included in our calculation.

Chalcopyrite solubility decreases with decreasing chloride concentration (Fig. 16b). For example, dissolved copper concentration decreases from 6 ppm in 5 m chloride solution to 0.4 ppm in 1 m chloride solution at 300 °C, which means that more than 90% of copper would precipitate as chalcopyrite from solution as chloride concentration decreases from 5 m to 1 m. Therefore, our calculations indicate that fluid mixing (dilution of saline fluids) can play a role for copper deposition from hydrothermal fluids.

6. CONCLUSIONS

The UV spectra of copper(I)-bearing LiCl solutions have been measured successfully at 100 °C–250 °C and chloride concentrations between 1.5 m and 9 m, a much wider range than can be used in conventional mineral solubility experiments. This technique enabled us to detect three copper(I)–chloride complexes important at high chloride concentrations and derive their formation constants. Interpretation of the spectral data yields the following conclusions.

1. This study demonstrates the usefulness of combining experimental methods to provide independent verification of formation constants as well as allowing wide ranges of temperature, pressure, and particularly ligand concentrations to be studied effectively.
2. This study confirms high-temperature formation constants for $CuCl_2^-$ derived from recent solubility experiments of Liu et al. (2001) and Xiao et al. (1998).
3. The formation constants for $CuCl_3^{2-}$ derived in this study are more reliable than those from previous experimental studies because we were able to study copper complexes at higher chloride concentrations than were used in the mineral solubility experiments.
4. This study provides the first direct experimental evidence that $CuCl_4^{3-}$ is an important complex at chloride concentrations greater than 6 m at temperatures between approximately 100 °C and 250 °C.

Table 6. Recommended logarithm of formation constants (log K) for copper(I) complexes.

Temperature	25 °C	50 °C	100 °C	150 °C	200 °C	250 °C	300 °C	350 °C
$Cu^+ + Cl^- = CuCl_{(aq)}$	4.17	3.99	3.81	3.76	3.81	3.97	4.28	5.01
$Cu^+ + 2Cl^- = CuCl_2^-$	5.46	5.30	5.13	5.10	5.16	5.32	5.63	6.34
$Cu^+ + 3Cl^- = CuCl_3^{2-}$	4.75	4.40	3.95	3.73	3.67	3.77	4.08	4.94
$Cu^+ + 4Cl^- = CuCl_4^{3-}$	2.77	2.14	1.42	1.16	1.23	1.63	2.51	4.67

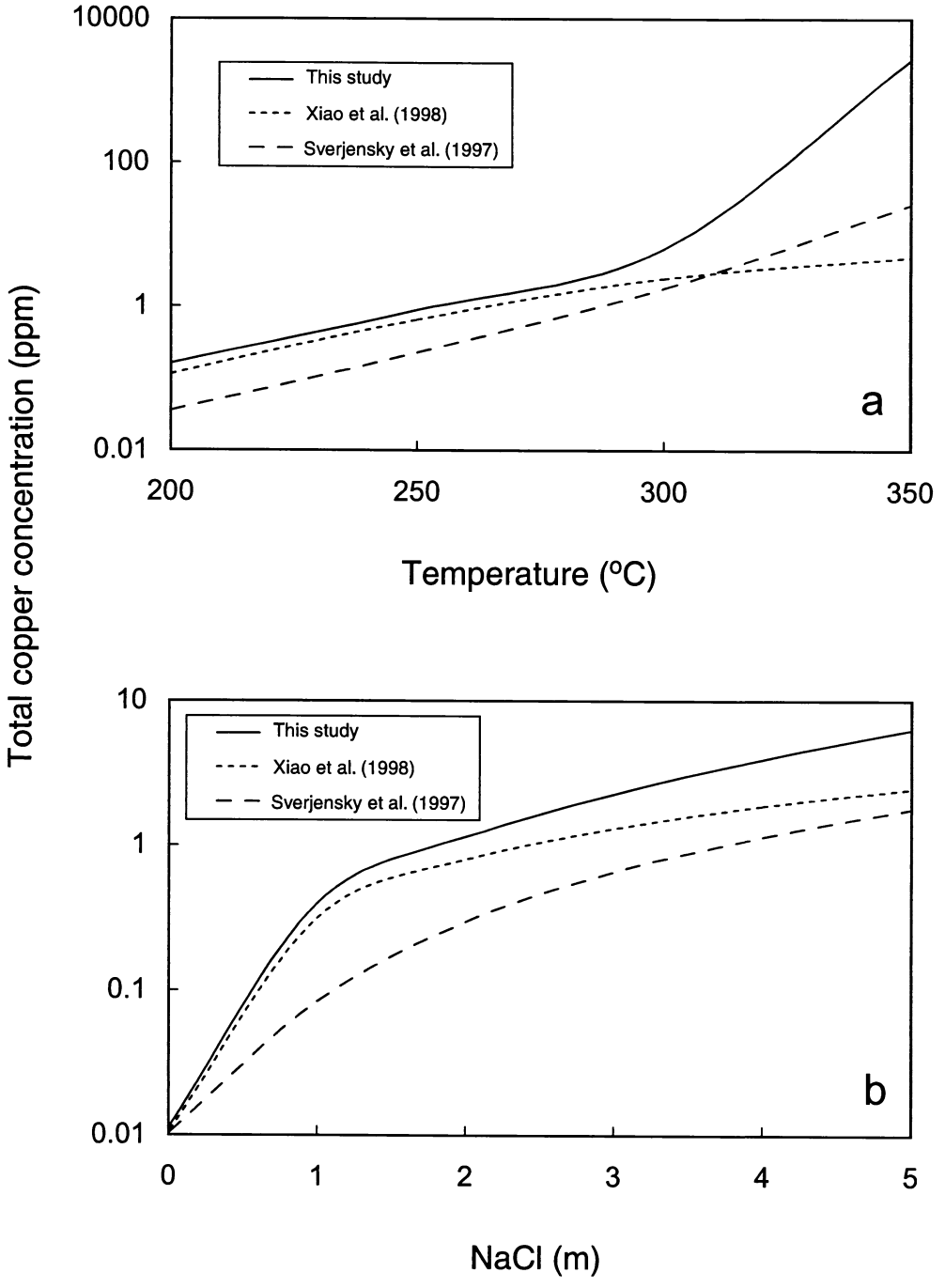

Fig. 16. Calculated chalcopyrite solubility in NaCl solutions in equilibrium with hematite–magnetite–pyrite: (a) Temperature between 200 °C and 350 °C and 1 m NaCl; (b) temperature = 300 °C and NaCl between 0.01 m and 5 m. The solid lines represent calculated solubilities using log K for copper(I)–chloride complexes derived from this study. The dashed and dotted lines stand for the values based on log K values for copper(I)–chloride complexes reported in Sverjensky et al. (1997) and Xiao et al. (1998), respectively.

5. Using the results of this study and Liu et al. (2001), calculations show that both cooling and fluid mixing are likely to be important in the deposition of copper from hydrothermal solutions.

The existence of $CuCl_3^{2-}$ and especially $CuCl_4^{3-}$ means that the solubilities of copper-bearing minerals are sensitive to changes in chloride concentration in brines with high chloride concentrations. The thermodynamic properties generated in this study, together with those of Liu et al. (2001) and Xiao et al. (1998), allow more reliable extrapolations of log K values for copper(I) complexes to high temperature and pressure, allowing more accurate numerical models of copper leaching, transport, and deposition in a wide range of hydrothermal environ-

ments such as porphyry copper ore deposits. Better understanding of the aqueous complexes of copper also allows more effective design of experiments and better interpretation of experimental and fluid inclusion data. This will be especially important in measuring and understanding the liquid–vapor partitioning of copper.

Acknowledgments—This paper is part of the first author's doctoral thesis. Thanks go to J. Black for setting up the dry glove box used in sample preparation. R. Shalders and C. Pierson are thanked for helping to design and build the pressure vessel used in this study. WL is grateful to Monash University for funding his Ph.D. scholarship. JB was funded by a fellowship from the Swiss National Science Foundation (credit 8220-056519). The research was funded by an Australian Research Council Large Grant to DCM. We thank E. H. Oelkers, A. E. Williams-Jones, and P. Bénézeth for their constructive and helpful comments.

Associate editor: E. H. Oelkers

REFERENCES

Ahrland S. and Rawsthorne J. (1970) The stability of metal halide complexes in aqueous solution VII. The chloride complexes of copper(I). *Acta Chem. Scand.* **24,** 157–172.

Anderson G. M., Castet S., Schott J., and Mesmer R. E. (1991) The density model for estimation of thermodynamic parameters of reactions at high temperatures and pressures. *Geochim. Cosmochim. Acta* **55,** 1769–1779.

Beane R. E. and Titley S. R. (1981) Porphyry copper deposits: Part II. Hydrothermal alteration and mineralization. *Economic Geology* **75**(Anniversary Volume), 214–269.

Bebie J., Seward T. M., and Hovey J. K. (1998) Spectrophotometric determination of the stability of thallium (I) chloride complexes in aqueous solution up to 200 °C. *Geochim. Cosmochim. Acta* **62,** 1643–1651.

Blandamer M. J. and Fox M. F. (1970) Theory and applications of charge-transfer-to-solvent spectra. *Chem. Rev.* **70,** 59–93.

Brugger J., McPhail D. C., Black J., and Spiccia L. (2001) Complexation of metal ions in brines: application of electronic spectroscopy in the study of the Cu(II)–LiCl–H_2O system between 25 and 90 °C. *Geochim. Cosmochim. Acta* **65,** 2691–2708.

Ciavatta L. and Iuliano M. (1998) Copper(I) chloride complexes in aqueous solution. *Annal. Chim.* **88,** 71–89.

Crerar D. A. and Barnes H. L. (1976) Ore solution chemistry V. Solubilities of chalcopyrite and chalcocite assemblages in hydrothermal solution at 200 to 300 °C. *Econ. Geol.* **71,** 772–794.

Davis D. D., Stevenson K. L., and Davis C. R. (1978) Photooxidation of dichloro- and trichlorocuprate(I) ions in acid solution. *J. Am. Chem. Soc.* **100,** 5344–5349.

De Juan A. and Tauler R. (1999) Multiple Curve Resolution Home Page (http://www.ub.es/gesq/mcr/mcr.htm).

De Juan A., Vander Heyden Y., Tauler R., and Massart D. L. (1997) Assessment of new constraints applied to the alternating least squares method. *Anal. Chim. Acta* **346,** 307–318.

Draper N. R. and Smith H. (1998) *Applied Regression Analysis*. Wiley-Interscience.

Fritz J. J. (1980) Chloride complexes of CuCl in aqueous solution. *J. Phys. Chem.* **84,** 2241–2246.

Fulton J. L., Hoffmann M., and Darab J. G. (2000a) An X-ray absorption fine structure study of copper(I) chloride coordination structure in water up to 325 °C. *Chem. Phys. Lett.* **330,** 300–308.

Fulton J. L., Hoffmann M. M., Darab J. G., and Palmer B. J. (2000b) Copper(I) and copper(II) coordination structure under hydrothermal conditions at 325 °C: an X-ray absorption fine structure and molecular dynamics study. *J. Phys. Chem. A* **104,** 11651–11663.

Gahler A. R. (1954) Colorimetric determination of copper with neocuproine. *Anal. Chem.* **26,** 577–580.

Glasner A. and Avinur P. (1961) Absorption bands of cuprous and cupric salts in concentrated alkali halide solutions, and their analytical implications. *Anal. Chem.* **33,** 1122–1123.

Hannington M. D., Jonasson I. R., Herzig P. M., and Petersen S. (1995) Physical and chemical processes of seafloor mineralization at mid-ocean ridges. In *Seafloor Hydrothermal Systems: Physical, Chemical, Biological, and Geological Interactions*, 91. (eds. S. E. Humphris, et al). Geophys. Monogr., 115–157.

Haynes D. W. (1986) Stratiform copper deposits hosted by low-energy sediments; II, Nature of source rocks and composition of metal-transporting water. *Econ. Geol.* **81,** 266–280.

Haynes D. W. and Bloom M. S. (1987a) Stratiform copper deposits hosted by low-energy sediments; III, Aspects of metal transport. *Econ. Geol.* **82,** 635–648.

Haynes D. W. and Bloom M. S. (1987b) Stratiform copper deposits hosted by low-energy sediments; IV, Aspects of sulfide precipitation. *Econ. Geol.* **82,** 875–893.

Heinrich C. A. and Seward T. M. (1990) A spectrophotometric study of aqueous iron(II) chloride complexing from 25 to 200 °C. *Geochim. Cosmochim. Acta* **54,** 2207–2221.

Helgeson H. C. (1969) Thermodynamics of hydrothermal systems at elevated temperatures and pressures. *Am. J. Sci.* **267,** 729–804.

Helgeson H. C. and Kirkham D. H. (1974) Theoretical prediction of the thermodynamic behavior of aqueous electrolytes at high pressures and temperatures; II, Debye-Huckel parameters for activity coefficients and relative partial molal properties. *Am. J. Sci.* **274,** 1199–1261.

Hemley J. J., Cygan G. L., Fein J. B., Robinson Jr. G. R., and D'Angelo W. M. (1992) Hydrothermal ore-forming processes in the light of studies in rock-buffered systems. I, Iron-copper-zinc-lead sulfide solubility relations. *Econ. Geol.* **87,** 1–22.

Hezarkhani A. and Williams-Jones A. E. (1998) Controls of alteration and mineralization in the Sungun porphyry copper deposit, Iran; evidence from fluid inclusions and stable isotopes. *Econ. Geol.* **93,** 651–670.

Hezarkhani A., Williams-Jones A. E., and Gammons C. H. (1999) Factors controlling copper solubility and chalcopyrite deposition in the Sungun porphyry copper deposit, Iran. *Miner. Depos.* **34,** 770–783.

Hikita H., Ishikawa H., and Esaka N. (1973) Solubility and equilibrium of copper(I) chloride in hydrochloric acid solutions. *Nippon Kagaku Kaishi* **1973,** 13–18.

Holmes H. F. and Mesmer R. E. (1983) Thermodynamic properties of aqueous solutions of the alkali metal chlorides to 250 °C. *J. Phys. Chem.* **87,** 1242–1255.

Hull S. and Keen D. A. (1994) High-pressure polymorphism of the copper(I) halides: A neutron-diffraction study to ~10 GPa. *Phys. Rev.* **50,** 5868–5885.

Johnson J. W., Oelkers E. H., and Helgeson H. C. (1992) SUPCRT92; a software package for calculating the standard molal thermodynamic properties of minerals, gases, aqueous species, and reactions from 1 to 5000 bar and 0 to 1000 °C. *Comput. Geosci.* **18,** 899–947.

Kau L.-S., Spira-Solomon A. J., Penner-Hahn J. E., Hodgson K. O., and Solomon E. I. (1987) X-ray absorption edge determination of the oxidation state and coordination number of copper: Application to the type 3 site in *Rhus vernicifera* laccase and its reaction with oxygen. *J. Am. Chem. Soc.* **109,** 6433–6442.

Keller R. N. and Wycoff H. D. (1946) Copper(I) chloride. In *Inorganic Syntheses*, Vol. 2. (ed. W. C. Fernelius). McGraw-Hill, pp. 1–4.

Kielland J. (1937) Individual activity coefficients of ions in aqueous solutions. *J. Am. Chem. Soc.* **59,** 1675–1678.

Lemmon E. W., McLinden M. O., and Friend D. G. (2000) Thermophysical properties of fluid systems. In *NIST Chemistry WebBook, NIST Standard Reference Database*, Vol. 69. (eds. W. G. Mallard and P. J. Linstrom). National Institute of Standards and Technology (http://webbook.nist.gov).

Liu W., McPhail D. C., and Brugger J. (2001) An experimental study of copper(I)–chloride and copper(I)–acetate complexing in hydrothermal solutions between 50 °C and 250 °C and vapor-saturated pressure. *Geochim. Cosmochim. Acta* **65,** 2937–2948.

Majer V., Inglese A., and Wood R. H. (1989) Volumetric properties of $LiCl_{(aq)}$ from 0.05 to 3.0 mol.kg^{-1}, 322 to 550 K, and 0.8 to 32.6 MPa. *J. Chem. Thermodyn.* **21,** 321–329.

Malinowski E. R. and Howery D. G. (1980) *Factor Analysis in Chemistry*. Wiley.

Mountain B. W. and Seward T. M. (1999) The hydrosulphide/sulphide complexes of copper(I): Experimental determination of stoichiometry and stability at 22 °C and reassessment of high temperature data. *Geochim. Cosmochim. Acta* **63,** 11–29.

Nelder J. A. and Mead R. (1965) A simplex method for function minimization. *Comput. J.* **7,** 308–313.

Nemaier A. (1998) MINQ_General definite and bound constrained indefinite quadratic programming. http://solon.cma.univie.ac.at/|P5neum/software/minq/.

Pfitzner A. and Lutz H. D. (1993) The systems CuCl–M(sup)IICl(sub)2 (M=Mn,Cd)-crystal structures of Cu(sub)2MnCl(sub)4 and γ-CuCl. *Z. Kristallogr.* **205,** 165–175.

Pokrovskii V. A. and Helgeson H. C. (1997) Calculation of the standard partial molal thermodynamic properties of KCl° and activity coefficients of aqueous KCl at temperatures and pressures to 1000 °C and 5 kbar. *Geochim. Cosmochim. Acta* **61,** 2175–2183.

Ran C., Liu W., Zhang Z., He M., and Chen H. (1995) Rifting cycle and storeyed texture of copper deposits and their geochemical evolution in Kandian region. *Sci. China (B)* **38,** 606–612.

Roedder E. (1984) *Fluid Inclusions*. Mineral Society of America.

Rose A. W. (1976) The effect of cuprous chloride complexes in the origin of Red-bed copper and related deposits. *Econ. Geol.* **71,** 1036–1048.

Ruaya J. R. (1988) Estimation of instability constants of metal chloride complexes in hydrothermal solutions up to 300 °C. *Geochim. Cosmochim. Acta* **52,** 1983–1996.

Setchénow M. (1889) Über die Konstitution der Salzlösungen auf Grund ihres Verhaltens zu Kohlensaure. *Z. Phys. Chem.* **4,** 117–126.

Seward T. M. (1976) The stability of chloride complexes of silver in hydrothermal solutions up to 350 °C. *Geochim. Cosmochim. Acta* **40,** 1329–1341.

Seward T. M. (1984) The formation of lead(II) chloride complexes to 300 °C; a spectrophotometric study. *Geochim. Cosmochim. Acta* **48,** 121–134.

Seyfried W. E. and Ding K. (1993) The effect of redox on the relative solubilities of copper and iron in Cl-bearing aqueous fluids at elevated temperatures and pressures: An experimental study with application to subseafloor hydrothermal systems. *Geochim. Cosmochim. Acta* **57,** 1905–1917.

Seyfried W. E. and Ding K. (1995) Phase equilibria in subseafloor hydrothermal systems: A review of the role of redox, temperature, *p*H and dissolved Cl on the chemistry of hot spring fluids at mid-ocean ridges. In *Seafloor Hydrothermal Systems: Physical, Chemical, Biological, and Geological Interactions*, 91. (eds. S. E. Humphris, et al). Geophys. Monogr., 248–272.

Sharma V. K. and Millero F. J. (1990) Equilibrium constants for the formation of Cu(I) halide complexes. *J. Sol. Chem.* **19,** 375–390.

Sugasaka K. and Fujii A. (1976) A spectrophotometric study of copper(I) chloro-complexes in aqueous 5M Na(Cl, ClO_4) solutions. *Bull. Chem. Soc. Jpn.* **49,** 82–86.

Sukhova T. G., Temkin O. N., Flid R. M., and Kaliya T. K. (1968) Determination of the composition and stability constants of chlorocuprate(I) complexes in concentrated solutions. *Russ. J. Inorg. Chem.* **13,** 1072–1076.

Sverjensky D. A. (1987) The role of migrating oil field brines in the formation of sediment-hosted Cu-rich deposits. *Econ. Geol.* **82,** 1130–1141.

Sverjensky D. A., Shock E. L., and Helgeson H. C. (1997) Prediction of the thermodynamic properties of aqueous metal complexes to 1000 °C and 5 kb. *Geochim. Cosmochim. Acta* **61,** 1359–1421.

Tauler R. and Casassas E. (1989) Application of principal component analysis to the study of multiple equilibria systems. Study of copper(II)/salicylate/mono-, di- and triethanolamine systems. *Anal. Chim. Acta* **223,** 257–268.

Tauler R. and Casassas E. (1992) Application of factor analysis to speciation in multiequilibria systems. *Analusis* **20,** 255–258.

Ulrich T., Guenther D., and Heinrich C. A. (1999) Gold concentrations of magmatic brines and the metal budget of porphyry copper deposits. *Nature (London)* **399,** 676–679.

Var'yash L. N. (1992) Cu(I) complexing in NaCl solutions at 300 and 350 °C. *Geochem. Int.* **29,** 84–92.

Von Damm K. L. (1995) Controls on the chemistry and temporal variability of seafloor hydrothermal fluids. In *Seafloor Hydrothermal Systems; Physical, Chemical, Biological, and Geological Interactions*, 91. (eds. S. E. Humphris, et al). Geophys. Monogr., 222–247.

Xiao Z., Gammons C. H., and Williams-Jones A. E. (1998) Experimental study of copper(I) chloride complexing in hydrothermal solutions at 40 to 300 °C and saturated water vapor pressure. *Geochim. Cosmochim. Acta* **62,** 2949–2964.

Zotov A. V., Levin K. A., Khodakovskiy I. L., and Kozlov V. K. (1986) Thermodynamic parameters of Ag(I) chloride complexes in aqueous solution at 273–623 K. *Geochem. Int.* **23,** 103–116.